The Dissertation Committee for Roger James Kapsimalis Certifies that this is the approved version of the following dissertation:

The Simultaneous Quantification of Fissile U and Pu Nuclides using Delayed Neutron Activation Analysis

Committee:

Sheldon Landsberger, Supervisor

Brian Anderson

Steve Biegalski

Alan Icenhour

Erich Schneider

The Simultaneous Quantification of Fissile U and Pu Nuclides using Delayed Neutron Activation Analysis

by

Roger James Kapsimalis, BSPhy; MSE

Dissertation

Presented to the Faculty of the Graduate School of

The University of Texas at Austin

in Partial Fulfillment

of the Requirements

for the Degree of

Doctor of Philosophy

The University of Texas at Austin

May 2013

Dedication

To that older couple who fed me for all those years,

Whatever successes I might achieve,
they are because of your support, love, and analogies.

Thanks, Mom and Dad.

Acknowledgements

There are several people whose support and expertise made this work possible. I would like to thank David Glasgow at the Neutron Activation Analysis Lab for all of his help developing this technique. I would also like to thank Dr. Ken Inn at NIST for graciously solving one of our biggest obstacles: finding plutonium reference material.

I am grateful to Drs. Alan Icenhour and Brian Anderson at ORNL for their support of this work and their feedback in its development. I would also like to thank my committee members Drs. Steve Biegalski and Erich Schneider, for helping with the formulation of this technique. Finally, I'd like to sincerely thank Dr. Sheldon Landsberger for his support of not only this work, but also his mentorship over the past several years.

The Simultaneous Quantification of Fissile U and Pu Nuclides using Delayed Neutron Activation Analysis

Roger James Kapsimalis, Ph.D.

The University of Texas at Austin, 2013

Supervisor: Sheldon Landsberger

The ability to quickly and accurately quantify fissile constituents in bulk materials remains essential to many aspects of nuclear forensics and for safeguarding nuclear materials and operations. This often entails the analysis of trace quantities of nuclear debris or effluents, and typically requires bulk sample digestion followed by actinide separation and mass spectrometry. Because destructive methods are time and labor intensive, efforts have been made to develop alternative nondestructive methods for this type of analysis. This work, performed at Oak Ridge National Laboratory at the High Flux Isotope Reactor (HFIR), seeks to utilize delayed neutron activation analysis on samples of interest containing multiple fissile constituents. Based on the variances in the fission product yields of individual fissile nuclides, this work utilizes methods of linear regression to derive a technique that allows for such analysis, forgoing chemical separation and using only a single irradiation and counting step.

Table of Contents

List of Tables

List of Figures

Chapter 1

Introduction

The continuing development of innovative analytical techniques remains the cornerstone of scientific efforts to prevent the proliferation of nuclear materials and to avert malevolent acts of nuclear aggression. These efforts consist of the collection, analysis, and interpretation of nuclear materials and debris. Current capabilities of the scientific community rely too greatly on analytical methods that provide data on timescales unacceptable for rapid-decision making. In light of this perceived deficiency in the current state of analytical capabilities, this work formulated a novel, rapid, nondestructive analytical method, which would concurrently determine isotopic concentrations of multiple fissile nuclides present in special nuclear materials. To establish such a capability, this project revisited the notion that the highly sensitive method of delayed neutron activation analysis may in fact be applicable to samples containing more than just a single fissile component.

As nuclear technologies continue to expand in all parts of the world, so increases the threat of nuclear proliferation and nuclear terrorism. A multinational effort to ensure the protection and security of nuclear materials and facilities has been advanced by both scientific discoveries and diplomatic initiatives. Institutional barriers against the proliferation of nuclear materials, specifically those implemented by the International Atomic Energy Agency (IAEA), have led to a myriad of multinational agreements,

treaties and increased international cooperation with strides made towards the disarmament of nuclear weapons across the globe. However, concerns over the strength of the Treaty on the Non-Proliferation of Nuclear Weapons have questioned the fortitude of nonproliferation policy and the very survival of the current international agreements (1) (2). Taking into account these concerns, as well as recent interest of non-weapons states to acquire nuclear arms, and the ever-present threat of a subnational or terrorist organization to acquire nuclear material, additional safeguards must be in place in order to maintain adequate control of nuclear material and to account for material in the event of theft, diversion, or sabotage (3). In the event that diplomatic efforts fail to prevent the diversion of nuclear material by maintaining control and accountability of fissile material (4) (5), scientific capabilities are needed to ensure timely attribution. Whether tasked with evaluating processes effluents, interdicted bulk nuclear materials, or debris following the detonation of a nuclear weapon, the scientific community is responsible for identifying the origin of the nuclear material quickly and accurately.

Described here is a novel approach to determining fissile isotopic concentrations, using a variation of delayed neutron activation analysis. Typical applications of DNAA measure the total number of delayed neutrons emitted from an irradiated sample, a quantity that is proportional to the concentration of fissile material in a sample. However, it will be shown that the masses of individual fissile nuclides can be ascertained from a single delayed neutron emission profile of an irradiated sample containing multiple fissile components, without chemical separation prior to analysis.

1.1 Nuclear Forensics

Nuclear forensics is a multidisciplinary, multifaceted scientific field tasked with the characterization of nuclear materials and the identification of key particularities that ultimately allow for the attribution of interdicted materials or sampled debris, as well as to decry illicit nuclear operations (6) (7). Bulk quantities of illicit nuclear materials have been intercepted at an alarming rate since the fall of former Soviet Union, indicating that an illegal market of stolen nuclear material exists today (8). Aside from these intercepted bulk materials, trace and ultra-trace concentrations of nuclear materials are often collected by environmental sampling techniques. The IAEA has implemented protocols to routinely monitor the controlled and uncontrolled releases of gaseous and aerosolized particulate matter from nuclear facilities as a safeguards verification technique (9) (10). The small quantities of particulate matter released during nuclear activities are collected by IAEA inspectors, primarily by swiping the surfaces of nuclear processing facilities. The bulk analysis of these samples containing trace amounts of nuclear materials is an especially important deterrent to state-sponsored undisclosed nuclear actions (11). The remote and onsite environmental sampling and subsequent sampling of nuclear facilities around the world remains a primary method of the IAEA's efforts to monitor and safeguard nuclear activities; the auditing of nuclear fuel processing, reprocessing, and enrichment facilities helps to ensure treaty compliance and to uncover clandestine operations.

Nuclear materials are characterized by their physical morphology (12), chemical composition (13), trace element contamination (14), isotopic composition (15), and many

other characteristics. However, the fundamental characteristic of any nuclear material is the concentration and isotopic ratios of its fissile components. Therefore, the ability to quickly and accurately quantify and characterize the fissile constituents in bulk nuclear materials is paramount to the safeguarding of nuclear materials, and to ensure the compliance of nuclear facilities.

Both large quantities of special nuclear material, and trace quantities collected in routine sampling efforts require destructive analytical methods for the determination of isotopic concentrations of the fissile nuclides present in the material. Consequently, this analysis, while very sensitive, often proves to be difficult and time-consuming task, as it involves chemical destruction and actinide separation for routine analysis (16) (17).

1.2 Current Analytical Methods

A limitation of the current analytical techniques is the inherently difficult nature of destructive analysis of nuclear materials, which often entails mass spectrometry preceded by extensive sample preparation. On one hand, mass spectrometric techniques remain the gold-standard today, however, these methods are time consuming and scenarios exist in which rapid decisions must be made regarding responsive actions, based on the composition and origin of the collected materials. Consequently, efforts have been made to develop alternative or complementary methods for the simultaneous quantification of uranium and transuranic nuclides within a given sample. It is therefore proposed that an analytical method utilizing DNAA be established as a method of

providing a baseline assessment of the concentrations of different fissile constituents present in a given sample. Ultimately, this will prove to be an invaluable technique that allows for accurate, yet timely, evaluation of nuclear materials. Because DNAA is not sensitive to matrix interferences (18) that other analytical techniques, including the mass-interferences that hinder mass spectrometric analysis, this technique will be well suited for both environmental samples and the assay of large quantities of intercepted illicit nuclear materials. A large neutron source, however, is required.

Delayed neutron activation analysis is a process in which neutron irradiation induces fission in the fissile constituents of a given sample. The neutron-rich fission products decay via the βn-mechanism and the fissile contents are quantified by the emission rate of the delayed neutrons. It is a long-established analytical technique; delayed neutron counting experiments date as far back as the late 1940's (19). Because DNAA is able to provide a fast, nondestructive method of determining trace-level fissile materials, regardless of the sample medium, it is used today with great success for a multitude of applications, including the determination of uranium content in environmental samples (20). Recently, there has been a resurgence of interest in using DNAA in the field of nuclear forensics, as it is recognized as a rapid alternative to other analytical methods including mass spectrometry and alpha spectroscopy (21).

However, DNAA is not currently applied to the analysis of materials containing two or more fissile nuclides because this technique fails to differentiate between fission caused by different nuclides. This is especially problematic for samples of interest that contain derivatives of discharged nuclear fuel containing fissile isotopes of both uranium

and plutonium. This work seeks to utilize DNAA to quantify multiple fissile nuclide systems without the sample preparation or chemical separation that hinders other techniques by exploiting the subtle differences in the βn-decay of fission products of different nuclides. This will ultimately allow for the deconvolution of the time-dependent neutron spectrum following sample irradiation.

1.3 Motivation

The primary motivation for this work, particularly at the onset of this project, was to address the analytical needs in determining isotopic concentrations of materials collected by environmental sampling efforts. One of the primary tasks of the Neutron Analysis Laboratory at the High Flux Isotope Reactor (HFIR) is to evaluate environmental swipe samples collected by the IAEA at nuclear materials processing facilities. These swipe samples provide valuable insight to the processes conducted at a facility and are paramount in the assurance of treaty compliance and the deterrence of illicit or covert operations. In particular, these swipes determine the isotopic concentrations of fissile ^{235}U to ensure that uranium is not being enriched to levels greater than declared limits. The current capabilities of the DNAA facility at HFIR and at other laboratories over the world are limited by the fact that current applications of DNAA cannot be used if more than a single fissile nuclide is present in the sample. If any of these materials contained a fissile component in addition to the uranium collected, the resultant measurements would be false. Additionally, it behooves the scientific

community to develop technologies to identify instances when more one fissile material is collected via swipe sampling, as this would indicate undeclared spent fuel reprocessing or other nuclear process. By developing a method that can identify secondary or tertiary fissile nuclides collected by IAEA swipe sampling, covert nuclear materials processes can be quickly and easily identified.

As this work progressed, the need for a nondestructive method of evaluating the fissile constituents of nuclear materials became increasingly apparent because of the potential breadth of information that could be gained from the analysis. Many of the basic characteristics of a nuclear material can be ascertained simply by the presence and relative concentrations of ^{235}U and ^{239}Pu. These fissile isotopes are of primary interest and greatest concern from a nonproliferation and nuclear forensics aspect because of their potential for direct-use in nuclear weapons.

Applications of a direct method of measuring the $^{239}Pu/^{235}U$ ratio in trace concentrations of nuclear material primarily include the analysis of materials actively or passively collected for nuclear safeguards practices. In addition to measuring isotopic ratios in swipe collections taken at uranium enrichment facilities to ensure compliancy, debris and process effluents collected via wide-area monitoring can be analyzed for ^{239}Pu contaminants to identify nuclear fuels separations or reprocessing facilities. Further still, this method would be of great value in the event of a nuclear accident, where the characterization of nuclear contaminants must be performed quickly and for a large number of collected materials.

1.4 Scope of Work

Because DNAA is a powerful nondestructive analytical method, with the capability to quantifying fissile material on the sub-nanogram level in a matter of minutes, without chemical or preparation or separation, described here is a method, which will allow for the concurrent determination of multiple fissile nuclides. This will broaden the applicability of DNAA to the assay of materials from all stages of the nuclear fuel cycle.

In order to develop a method that allows for samples containing two or more fissile constituents to be analyzed, the time-evolution of the delayed neutron emission profile of an irradiated material had to be considered. Each fissile nuclide has a unique fission product yield. Because of the differences in fission products, and their half-lives, of different fissile nuclides, each fissile nuclide has a unique delayed neutron emission profile. By empirically developing explanatory functions, or *basis functions*, that describe the time-dependent delayed neutron emission profile per unit mass for each individual fissile nuclide of interest, methods of linear regression were used to deconvolve the delayed neutron spectrum of a sample containing multiple fissile nuclides.

The experimental work performed to establish this technique consisted of first building an appropriate neutron counting system. The Neutron Activation Analysis Laboratory at Oak Ridge National Laboratory (ORNL) is routinely used for the analysis of a broad spectrum of samples, including IAEA swipe samples that are analyzed for uranium content and enrichment using a combination of DNAA and neutron activation

analysis (NAA) with subsequent gamma-ray spectrometry; however, before the onset of this project, the system was not capable of resolving a time-dependent neutron spectrum. Therefore, several modifications were made to the existing counting system at HFIR. These included the replacement of many analog components and the installation of a computer-interfaced multichannel scaler. A thorough description of the system and the improvements made is provided in a Chapter 5 of this paper.

Once these enhancements to the neutron counting system were made, samples were prepared for irradiation by diluting standard reference materials that contained certified uranium and plutonium isotopic concentrations.

Samples were irradiated using the 85 MW High Flux Isotope Reactor (HFIR) at ORNL. HFIR was advantageous for two primary reasons. First, the immense neutron flux, $4x10^{13}$ $n.cm^{-2}s^{-1}$ in the irradiation position, allowed for a greater reaction rate and more induced fissions. Second, the irradiation position has a large thermal to fast flux ratio. This nearly thermal flux minimized any fast-neutron induced fission reactions of other nuclides, which would skew the results if not adequately accounted.

The bulk of this work came in terms of the data analysis and the ultimate quantification of each contributing fissile nuclide to the single acquired delayed neutron spectrum. A multi-element regression model was chosen to describe the delayed neutron emission profile following thermal irradiation of a sample containing multiple fissile nuclides. The detector response could then be expressed as an array of discrete neutron counts at a series of time steps. Consequently, the regression model could be used to determine the concentrations of each fissile nuclide present, providing that the predicted

detector response at each time step for each nuclide was known. This predicted response was then modeled as a basis vector. Isotopically certified reference materials were used to empirically characterize these basis vectors. Using linear regression techniques, the masses of each contributing nuclide were then found.

With a nondestructive method to concurrently measure multiple fissile nuclides, this work sought to characterize the method and the system in place at ORNL. Experiments were conducted to evaluate and optimize lower limits of detection and to improve the fidelity of the collective parametric quantities empirically found in the regression model.

Chapter 2

Isotope Ratio Analysis: A Literature Review

While the field of nuclear forensics employs a wide variety of analytical methods to determine the physical, chemical, and radiological properties of special nuclear materials and their derivatives, the isotopic ratio analysis of these materials remains the pinnacle of all forensics efforts. These ratios can be used to positively identify the origin and history of a nuclear material; specifically, by focusing on the isotopic analysis of the uranium and plutonium nuclides present in a sample, the source material can be defined (22).

Analyzing the isotopic ratios of actinides present in a sample can shed light on numerous forensics questions regarding the material. These ratios can be used to attribute illicit materials (23) (24) (25), to analyze environmental samples for safeguards purposes (26) (27), or the assay of discharged nuclear fuel (28) (29) (30). Additionally, these ratios can be used to analyze debris following a detonation or nuclear accident (31).

The focus of this work is on the isotopic ratio analysis of special nuclear materials (SNM). As defined by both the IAEA and the United States Atomic Energy Act of 1954, special nuclear materials are those that pose grave risks in regards to their attractiveness for proliferation. Specifically, these materials are those containing quantities of plutonium and/or uranium enriched in either ^{233}U or ^{235}U fissile isotopes. The purpose of this chapter is to give an overview of isotopic ratio analysis, its applications, and its

importance in the characterization of special nuclear materials. An assessment of the current capabilities to perform such work is also offered.

2.1 Actinide Ratios of Significance

Isotope ratio analysis is a pillar of nuclear forensics efforts. It is used to identify materials and processes that can ultimately be used for the attribution of nuclear materials and debris. Current methods of isotope ratio analysis of nuclear materials consider not only key actinides for identification of specific nuclear processes parameters, but also trace isotopes, which can provide insight to the geographical origins of a material. The delayed neutron activation analysis developed in this work technique cannot, and even after extensive refinements, will not, be able to quantify more than a select few nuclides. While this is a disadvantage in comparison to mass spectrometry, the few nuclides that DNAA is capable of determining can provide a wealth of valuable information pertaining to the origin and intended use of a given nuclear material on a timescale much quicker than destructive analytical methods.

The importance of actinide ratio analysis can be realized at nearly every point of the nuclear fuel cycle. A fast, accurate method of determining these isotopic ratios can ultimately be used for many practical purposes, pursuant to the proper handling, safe storage, and security of nuclear materials. Precisely which ratios are important and what practical information can be ascertained from these measurements will be discussed

below, bearing particular importance to ratios that serve as radio "fingerprints" that can be used to identify specific chemical or nuclear processes.

The nuclear fuel cycle can be discretized into three major components: the front end, the service period, and the back end. During each period, the composition of the nuclear material drastically changes. Actinide compositions of nuclear material can be a strong indicator as to a material's intended use and the processes used to create it. Consequently, actinide ratios can be used to determine the origin of an unknown material, or to monitor the processes used to formulate them.

Special nuclear material is introduced into the fuel cycle during uranium enrichment. In an effort to prevent nuclear proliferation, the IAEA routinely monitors the production of enriched uranium and to identify clandestine operations at enrichment facilities. The isotopic ratios of enriched uranium, uranium tails, and process effluents serve as an indicator of treaty compliance. The detection of covert HEU production remains the primary safeguards objective at any enrichment facility (32) and environmental sampling is the preferred method of collection to ensure that highly enriched uranium is not being produced. Particulates formed by the hydrolysis of UF_6 released during normal operations (33) are collected by inspectors and analyzed for isotopic signatures. The $^{235}U/^{238}U$, which can be found by delayed neutron activation analysis followed by gamma-spectroscopy, is the primary indicator of clandestine highly enriched uranium production at nuclear facilities

During the service period of the nuclear fuel cycle, plutonium is introduced into the material matrix. ^{239}Pu production, by neutron capture of ^{238}U, provides a wealth of

information pertaining to many reactor specific parameters, including burn up and initial fuel composition. Interdicted material, which had been intentionally diverted from discharged nuclear fuel, could potentially be traced back to a specific reactor design using actinide ratios. Concurrently uranium and plutonium measurements can provide several isotopic ratios of significance and identify material that has been derived from the service period of the nuclear fuel cycle. The $^{239}Pu/^{235}U$ and $^{241}Pu/^{235}U$ ratios identify burnup parameters that can be used to characterize an illicit material. The determination of other trace fissile Am and Cm nuclides can also be used to identify specific reactor types or initial fuel composition, all of which can provide clues as to the origin of an interdicted material. Additionally, because of the short half-life of ^{241}Pu, the $^{241}Pu/^{239}Pu$ ratio can be used to easily date an unknown plutonium-bearing material.

Finally, debris and effluents can be collected and categorized using fissile isotope measurements. Currently, atmospheric sampling is used to detect clandestine nuclear fuel separation and reprocessing facilities. Using aerosol samplers, collections are made over long periods of time (on the order of weeks or longer) to collect effluents that may have been released during operations within 100 km (34). As such, uranium and plutonium isotopic ratios are used to differentiate effluents from atmospheric fallout. In the event of a nuclear detonation or large-scale nuclear accident, plutonium isotopic ratios can be used in the attribution of a material, but can also be used to determine the yield of a nuclear detonation.

2.2 Determination of Isotopic Ratios

Uranium and plutonium isotopic ratio analysis, particularly in sample sets containing trace amounts of material, is most commonly performed using one form of mass spectrometry or another. First, a brief overview of this form of analysis follows, while details of the current techniques are described in subsequent pages.

The basic components of all mass spectrometry instruments include an ionization source, an extraction method, a mass-to-charge separator, and a detector system. The fundamental premise is that once ions are formed and injected into a mass analyzer, atoms or molecules can be separated spatially or temporally by their respective mass-to-charge ratio (35). The ions are collected by a detector array according to these separation parameters and quantitative measurements to the relative abundances of each charged particle can be made. Of the techniques discussed in greater detail, these methods vary primarily with respect to the method of ionization. Generally speaking, mass spectrometry is a very powerful technique and can be used to determine isotopic abundances of very minute quantities of material.

The current state-of-the art methods for the determination of isotopic ratios of actinides present in a given material include several mass spectrometric techniques, such as inductively coupled plasma mass spectrometry (ICP-MS), high-efficiency thermal ionization mass spectrometry (TIMS), resonance ionization mass spectrometry (RIMS, or accelerator mass spectrometry (AMS) (36) (37) (38) (39) (40) (41) (42) (43). These techniques are discussed in greater detail below, but it should be noted that all of these methods require sample destruction and actinide separation prior to analysis. While these

methods provide great sensitivity and high precision, they are limited by the time-consuming sample preparation. It has been suggested here and in the literature (44) (27) that time required for material collection and subsequent destructive analysis does not meet the timeliness criterion currently implemented by the IAEA for the detection of illicit materials production.

Thermal ionization mass spectrometry entails heating a chemically purified sample on a filament to the point of thermal desorption and ionization. While TIMS yields highly precise measurements, thermal ionization does not break apart molecular interferences as effectively as other ionization methods. As such TIMS is particularly susceptible to hydrocarbon interferences, limiting its applicability of analyzing mixed uranium and plutonium samples (45). Once the actinides are separated from the sample matrix and analyzed, TIMS provides uranium detection limits on the order of 10 femtograms (46).

Resonance ionization mass spectrometry assuages many isobaric interferences, particularly in mixed actinide materials by using narrow bandwidth lasers to ionize and excite specific nuclides. Because individual elements have unique, discrete ionization energies, a finely tuned laser can be used to ionize only the analyte of interest. Results of this method show greater precision and accuracy for the determination of U and Pu (47) (48) than other spectrometric techniques using more traditional ionization sources.

Accelerator mass spectrometry has also been shown to be on the cutting edge of uranium and plutonium isotopic analysis, due to its low susceptibility to matrix interferences (49). By using a tandem electrostatic accelerator to accelerate ions and

dissociate atoms, isotopic, isobaric, and molecular interferences are reduced by several orders of magnitude (50). Detection limits have been shown to be on the order of 10^6 atoms for plutonium analysis (51). Similar results have been shown for uranium isotopics as well.

Inductively coupled plasma mass spectrometry is one of the most widely used mass spectrometric techniques used today. Atomization and ionization is achieved by introducing the analyte to a high temperature plasma, which dissociates molecules and generate M^+ or M^{2+} ions. Detection limits for uranium and plutonium have been found to be on the order of 10^{-11} grams using ICP-MS; detection limits are improved by several orders of magnitude by introducing a multi-collector detection system to mitigate interferences.

There are of course methods alternative to mass spectrometry used today, albeit not with similar frequency. Nondestructive methods, such as passive gamma-ray spectrometry, are continually being investigated to serve as a viable method for uranium and plutonium isotopic analysis. However, because of the weak radioactivity of uranium and plutonium nuclides, even the most sensitive gamma-ray spectrometry systems are severely limited by necessary count times and sample mass. Alpha particle spectroscopy is also sometimes used for the determination of plutonium nuclides. However, sample preparation, which entails all of the destruction and chemical separation needed for mass spectrometry plus additional steps to create ultra-thin sample deposits to avoid self-shielding of the alpha particles, make this technique unappealing for most applications.

Finally, of course, there is delayed neutron activation analysis. DNAA has been utilized for more than half a century for the determination of ^{235}U in a variety of sample matrices. If followed by gamma-ray spectroscopy of the activated sample, $^{235}U/^{238}U$ ratios can be measured without the need for destructive sample preparation. This implementation of DNAA is routinely used at the Neutron Irradiation Facility at Oak Ridge National Laboratory and at facilities around the world. A variety of uranium-bearing samples, including IAEA environmental sampling swipes, are analyzed with this method; however, this approach fails if the analyte contain multiple fissile components. There has been speculation as to whether DNAA could potentially be modified to analyze samples containing more than one fissile constituent. To date, though, only a single paper has been published claiming to have successfully quantified samples containing two fissile components using delayed neutron activation analysis. Li, Henkelmann, and Baumgartner in Munich utilized the delayed neutron counting system at the FRM-II reactor to quantify binary mixtures of ^{235}U and ^{239}Pu (66). There are several similarities with the work performed at ORNL and this paper; however, several basic differences are also apparent. The similarities are discussed below, as are, more importantly, the key differences. The limited scope of the Li paper represents only a part of the work performed for this project.

The theory behind using delayed neutron activation analysis for the quantification of multiple fissile nuclides, as presented by Li, Henkelmann, and Baumgartner is remarkably similar to the theoretical explanation offered in Chapter 3 of this work. In short, both acknowledge that due to the different fission product yields for each fissile

nuclide, a unique time-dependent neutron emission profile can be produced following material irradiation. In addition, the Li *et al.* work too suggests that the measured delayed neutron emission profile can be somehow deconvoluted to quantify each contributing fissile component.

Li, Henkelmann, and Baumgartner performed irradiations at the FRM-II reactor, which has a thermal neutron flux several orders of magnitude less than that of the irradiation position used at HFIR for this work. The remaining experimental conditions were also similar, as both this work and theirs utilized a delayed neutron counting array of ^{3}He detectors and a multichannel scaler to acquire a usable neutron decay spectrum. However, the projects differ in the subsequent analysis of the neutron signal. The paper is quite ambiguous in terms of describing the methodology used to deconvolve the delayed neutron spectrum, but it seems that Li, Henkelmann, and Baumgartner took a sort of "curve fitting" approach where the neutron emission rate was fit to a curve of the form:

$$C = Xe^{-\alpha t} + Ye^{-\beta t} \quad (1)$$

where X and Y are the masses of each contributing fissile constituent and the exponentials are constants in some time domain acquired by irradiating 1 μg samples of each ^{239}Pu and ^{235}U.

While this "curve fitting" technique showed promising results for some of the higher-concentration binary mixtures, the Li *et al.* method of analysis was insufficient and generally lacking. This is certainly evident by the 20% errors quoted by the authors, which they over-simplistically attributed to "counting statistics". Li, Henkelmann, and Baumgartner seem to demonstrate that simply fitting the delayed neutron curve is a poor

technique that ultimately breaks down at low concentrations of fissile material. Further, the method of analysis would not be feasible to apply to materials that contain more than two fissile materials.

2.3 Conclusions

There is a wide range of analytical tools available to the nuclear forensics scientist for the analysis of nuclear materials. The physical, chemical, and radiological characteristics of a given nuclear material are all of great importance in the analysis of nuclear materials. Physical properties, such as surface morphology and structure are determined using a number of microscopic instruments, including optical microscopy and high resolution scanning electron microscopy (SEM) and transmission electron microscopy (TEM) (52) (53). Radiological properties are often surveyed by way of gamma-ray spectrometry and alpha spectrometry (54) (55). Chemical compositions are determined a number of different ways, using energy-dispersive X-ray analysis (EDX) for example (3). However, it is the advent of high-resolution mass spectrometric techniques that have allowed for the precise measurements of chemical and isotopic compositions of nuclear materials (56). Currently, the choice method in fissile isotope quantification in special nuclear materials remains inorganic mass spectrometric techniques; ICP-MS is currently one of the single most powerful tools for nuclear forensic applications (3).

Inorganic mass spectrometry is used often in both the determination of trace amounts of material in environmental samples (57), as well as to determine isotopic ratios

in bulk nuclear materials (58). The challenges of mass spectrometric techniques arise in the required sample preparation associated with the destructive chemical separations performed prior to analysis. In order to quantify actinides in either bulk nuclear material or trace-concentrations collect by way of environmental sampling, the process beings with the destruction of both the sample material and its collection matrix (59). This process is of course matrix-dependent, but for many instances involves the dry ashing of the sample. Acid digestion and then evaporation typically follows. Actinide separation is carried out by any number of methods; resin columns are common. The actinide concentrations are then determined by one of several high-precision instruments. Today, multi-collector inductively coupled plasma MS (MC-ICP-MS) and thermal ionization mass spectrometry (TIMS) offer the greatest sensitivities.

Mass spectrometry remains at the forefront of both research and application for the assay of nuclear materials. However, there remain limitations with regard to mass spectrometric techniques, and therefore there is great interest in novel approaches that could complement the existing destructive analytical methods.

Chapter 3

Basics of Delayed Neutron Activation Analysis

Delayed neutrons have been studied extensively since the 1940's due to their significance in nuclear chain reactions and nuclear reactor kinetics. Delayed neutrons have also been used for decades in the radioanalysis of fissile materials. While the underlying theory governing the proposed analysis may be unremarkable, it is the concurrent determination and quantification of multiple fissile nuclides that remains a novel and arduous task.

3.1 Neutron Activation Analysis

Neutron activation analysis can be summarized as a three step analytical process involving sample preparation, irradiation, and activation-product counting.

The samples of greatest analytical interest to this work are those taken from environmental swipe sampling. The IAEA uses environmental swipes as an integral part of routine inspections, and environmental swipes are a key forensic sampling method of nuclear materials (11). The primary motivating factor in employing delayed neutron counting for this work, as opposed to the commonly used destructive analytical techniques, is of course the benefit of sample preparation. In this light, this work will

forgo any sort of actinide concentration, which typically involves ashing of the sample followed by chemical dissolution (60).

Samples were prepared at Oak Ridge National Laboratory using methods consistent with swipes collected by IAEA environmental sampling efforts. Samples of varying actinide composition were made in order to validate the method. Minimally, samples were prepared in such a manner that they contained variable concentrations of ^{235}U, ^{238}U, and ^{239}Pu. Sample irradiations were performed at ORNL using the onsite irradiation capabilities at HFIR. HFIR is a light water moderated, 85 MW reactor, which uses highly enriched uranium fuel. Consequently, HFIR provides one of the highest neutron fluxes of any research reactor in the world, and as such. Its thermal neutron flux of 4.0×10^{13} $n.cm^{-2}.s^{-1}$ allows for increased fission rates, and accordingly, greater fission product activation relative to other irradiation facilities. To increase the sensitivity of the delayed neutron counting, and thus achieve the lowest limits of detection, it is necessary to maximize the number of product precursor nuclides. The production rate of precursor nuclides is proportional to the fission rate of the sample (61).

$$P = \frac{R}{\lambda}\left(1 - e^{-\lambda t}\right) \quad (2)$$

where

λ is the decay constant of the precursor nuclide

t is the length of time that the sample is irradiated

R is the fission reaction given as

$$R = \frac{mN_A}{M}\sigma_f \phi \quad (3)$$

where

m is the mass of the fissile constituent

N_A is Avogadro's number

M is the atomic mass number of the fissile nuclide

σ_f is the thermal fission cross-section

ϕ is the thermal neutron activation flux

It is necessary to irradiate samples long enough to allow for adequate saturation of fission products before counting; as evident by Equations 2 and 3, the large thermal neutron flux provided in the HFIR irradiation facility increases the production rate of the delayed neutron precursors by more than an order of magnitude when compared to the activation of a sample in a 1 MW research reactor (62). It is also important to note that the irradiation position in HFIR is within its beryllium reflector, providing a nearly totally thermal neutron flux. Because there are only about 157 delayed neutrons released per 10^4 fission events (63), it is important to be able to increase the number of fission events as much as possible in order to acquire the most detailed βn signal for neutron counting.

Neutron activation analysis at HFIR is facilitated by two pneumatic transfer systems, PT-1 and PT-2. PT-2 was utilized for this work, as the transfer system terminates at the automated delayed-neutron counting array. The counting system consists of 18 ^{3}He neutron detectors to count isotropically emitted neutrons in the 2π direction. The sample transfer time between its irradiation position and counting position is roughly 2.5 seconds, which precludes analysis of the first delayed neutron group, according to the six-group approximation.

3.2 Delayed Neutrons

During a nuclear fission event, several free neutrons are released. Those neutrons released within 10^{-13} seconds of the splitting of the nucleus, are termed *prompt neutrons*. *Delayed neutrons*, however, are the result of fission products undergoing neutron emission associated with β-decay. The β-decay of the precursor nuclide leaves the radiogenic daughter product in an energy state higher than that of the neutron binding energy, thus causing the emission of a neutron. The first delayed neutrons begin to appear at roughly 10^{-1} seconds following fission, but most precursor nuclides have considerable half-lives; consequently, most delayed neutrons take considerably longer to appear. Of the hundreds of nuclides formed following the fission of actinides, there are roughly 40 fission products, of varying half-lives, that decay via βn-decay (64).

Due to the increasing neutron:proton ratio as a function of increasing atomic number, the atomic fragments following fission are almost always neutron rich. As such, these fission products undergo β-decay at a rate proportional to their deviation from nuclear stability. Following β-decay the daughter product exists at some energy, equal to Q_β, above its ground state. If Q_β is greater than the binding energy of the neutron, S_n, then the nuclide may undergo subsequent neutron emission, as illustrated below in Figure 1.

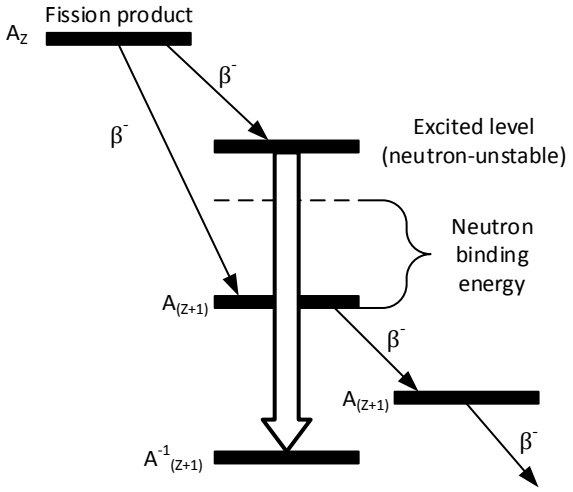

Fig. 1. Energy diagram of delayed neutron precursor
followed by delayed-neutron emission (63)

The probability that a particular nuclide will emit a neutron as a result of βn-decay is proportional to

$$Q_\beta - S_n \qquad (4)$$

As will be seen, the number of delayed neutrons emitted following the irradiation of a fissile material is proportional to the initial concentration of fissile nuclides. This is the basis for delayed neutron activation analysis.

3.3 Delayed Neutron Activation Analysis

Delayed neutron activation analysis is routinely performed at the Neutron Irradiation Facility at ORNL, and several other facilities across the world, for the determination of ^{235}U in a variety of matrices, including environmental swipe samples.

Classically, DNAA uses a comparator method to quantify the concentration of ^{235}U in a given sample by irradiating a known standard and counting the total number of delayed neutrons emitted from the sample for a prescribed length of time. Under identical irradiation and counting parameters, the ratio of the number of neutrons emitted from the unknown sample to the known sample can be used to determine the mass of the ^{235}U present.

While this implementation of DNAA has been well suited for quantifying fissile uranium in a wide range of materials, with detection limits on the order of picograms without the need for chemical preparation or separation, the comparator method fails if the sample has multiple fissile nuclides present. This stipulation limits the applicability of DNAA in the field of nuclear forensics, where samples may contain multiple fissile nuclides including ^{235}U, ^{239}Pu, as well as heavier fissile plutonium nuclides and some americium and curium nuclides.

Fundamentally, delayed neutron counting measures the neutron emission from a given sample as a function of time. The number of neutrons emitted from a sample is proportional to the number of fission products formed, which is to say that the initial concentration of fissile material can be determined by the number of delayed neutrons counted. The neutron intensity as a function of time can be described as the summation of the decay of the neutron precursor.

$$s = n_f \sum_{k=1}^{N} \nu_{d_k} \lambda_k e^{-\lambda_k t} \quad (5)$$

where

N is the number of delayed neutron precursors

n_f is the number of atoms that undergo fission in a sample

λ is the precursor group constant

Rarely are delayed neutrons counted in such a manner, but rather are grouped depending on the half-life of each delayed neutron precursor. Equation 5 can be vastly simplified by using the six-group delayed neutron model to describe the total neutron source rate. By doing so, equation 5 can be written as follows

$$s = n_f \sum_{k=1}^{6} \nu_{d_k} \lambda_k e^{-\lambda_k t} \quad (6)$$

where

ν_d is the delayed neutron fraction of each delayed neutron precursor group

The summation is taken over the number of groups, typically six, as is shown in equation 6.

The delayed neutron yield varies depending on the nuclide undergoing fission. Table 1 summarizes the total and delayed neutron yield of nuclides, which undergo thermal fission and are of particular interest to this work. The delayed neutron fraction is defined as simply the ratio of delayed neutrons to the total number of neutrons emitted during fission.

$$\beta = \frac{delayed\ neutrons}{delayed\ neutrons + prompt\ neutrons} \quad (7)$$

Table 1. Neutron yields of key fission precursors. Adapted from (65)

Nuclide	Total Neutron Yield	Delayed-Neutron Yield	Delayed-Neutron Fraction
^{235}U	2.4355 +/- 0.0023	0.0162 +/- 0.0005	0.0066
^{239}Pu	2.8836 +/- 0.0047	0.0065 +/- 0.0003	0.0022

The delayed neutron groups are characterized in the six-group model by their respective half-lives. The half-lives of the precursor groups range from roughly 0.2 s to 55 s. Figure 2, below, shows the time-dependent decay of the individual precursor groups following the thermal irradiation of ^{235}U.

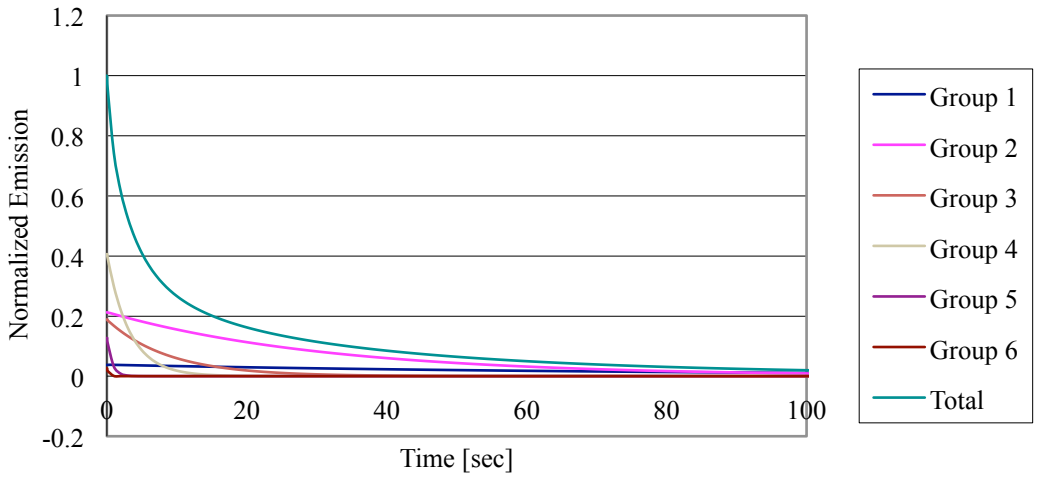

Fig. 2. Decay of six precursor groups of ^{235}U

The differences in fission product yield and consequently differences in delayed neutron precursor groups for the above mentioned nuclides are summarized below. These differences will be exploited in order to simultaneously quantify unique fissile nuclides in samples using delayed neutron counting.

Table 2. Delayed neutron group parameters

Group	**Average Half-life [s]**		**Delayed Neutron Fraction [%]**	
	^{239}Pu	^{235}U	^{239}Pu	^{235}U
1	54.28	55.72	0.0072	0.0210
2	23.04	22.72	0.0626	0.1400
3	5.60	6.22	0.0444	0.1260
4	2.13	2.30	0.0685	0.2520
5	0.62	0.61	0.0180	0.0740
6	0.26	0.23	0.0093	0.0270

With the above group parameters, an expression of the total delayed neutron source rate can be given as the sum of the delayed neutron source rates of each fissile nuclide present in the sample as

$$s_d = \sum_{i=1}^{N} n_{f_i} \sum_{k=1}^{6} \nu_{d_{ki}} \lambda_{ki} e^{-\lambda_{ki} t} \quad (8)$$

where

N is the number of fissile constituents present in the sample

n_{f_i} is the number of atoms, of isotope *i*, which undergo fission

$\nu_{d_{ki}}$ is the delayed neutron yield, in the k^{th} decay group, of nuclide *i*

λ_{ki} is the decay constant of the k^{th} decay group, of nuclide *i*

The difference in the neutron group parameters correlates to each fissile nuclide producing a different-shaped delayed neutron intensity profile. These individual neutron intensity-time curves are the consequence of variances in fission product yields in the precursor groups.

3.4 Spectra Formulation

The time-dependent neutron counting rate can be expressed as

$$c(t) = \varepsilon \sum_{i=1}^{N} \frac{m_i N_A}{M} \sigma_f \phi (1 - e^{-\lambda_i t_s}) \sum_{k=1}^{6} \nu_{d_{ki}} \lambda_{ki} e^{-\lambda_{ki} t_c} \quad (9)$$

where

ε is the neutron counting efficiency

m is the mass of the i^{th} fissile

N_A is Avogadro's number

M is the atomic mass number of the i^{th} fissile nuclide

σ_f is the fission cross-section

ϕ is the thermal neutron activation flux

Equation 9 can be expressed as the count rate per unit mass, *P(t),* multiplied by the mass of the constituent nuclide (66).

$$c(t) = \sum_{i=1}^{N} P_i(t) \cdot m_i \quad (10)$$

The detector response, *c(t)*, can be thought of as the sum of a series of points given as

$$c_i = c(t_i \pm \delta/2) \quad (11)$$

where

δ is the detector dwell time.

Of course, by reducing δ, the efficiency of the detector system increases and the delayed neutron counting statistics improve proportionally. The detector response at a given point, c_i, is total neutrons from the βn-decay of precursor nuclides from the fission of each fissionable nuclide present in the sample.

$$c_i = c_\alpha + c_\beta + c_\gamma \ldots + c_\omega \quad (12)$$

where subscripts α, β, γ,…, ω are contributing fissionable nuclides

Equation 12 can be expressed in terms of its count rate per unit mass for each nuclide, as was done above.

$$P^\alpha(t_i \pm \delta) \cdot m_\alpha + P^\beta(t_i \pm \delta) \cdot m_\beta + P^\gamma(t_i \pm \delta) \cdot m_\gamma + \cdots + P^\omega(t_i \pm \delta) \cdot m_\omega \quad (13)$$

For a sample initially containing four basis functions, which include the four possible fissile constituents in the sample, the detector response at point c_i would be given by the following expression.

$$c_i = P^\alpha(t_i \pm \delta) \cdot m_\alpha + P^\beta(t_i \pm \delta) \cdot m_\beta + P^\gamma(t_i \pm \delta) \cdot m_\gamma + P^\delta(t_i \pm \delta) \cdot m_\delta \quad (14)$$

The total count rate of the neutron detector can be expressed as a linear combination of points c_1 to c_i. This is best represented in the following matrix.

$$\begin{bmatrix} c_1 \\ \vdots \\ c_i \\ \vdots \\ c_\eta \end{bmatrix} = \begin{bmatrix} P^\alpha(t_1 \pm \delta) & P^\beta(t_i \pm \delta) & P^\gamma(t_1 \pm \delta) & P^\delta(t_1 \pm \delta) \\ \vdots & \vdots & \vdots & \vdots \\ P^\alpha(t_i \pm \delta) & P^\beta(t_i \pm \delta) & P^\gamma(t_i \pm \delta) & P^\delta(t_i \pm \delta) \\ \vdots & \vdots & \vdots & \vdots \\ P^\alpha\left(t_\eta \pm \delta\right) & P^\beta\left(t_\eta \pm \delta\right) & P^\gamma\left(t_\eta \pm \delta\right) & P^\delta(t_\eta \pm \delta) \end{bmatrix} \cdot \begin{bmatrix} m_\alpha \\ m_\beta \\ m_\gamma \\ m_\delta \end{bmatrix} \quad (15)$$

$$\boldsymbol{C} = (\boldsymbol{P_\alpha}, \boldsymbol{P_\beta}, \boldsymbol{P_\gamma}, \boldsymbol{P_\delta},) \cdot \boldsymbol{M} \quad (16)$$

The parameters $\boldsymbol{P_i}$ are known from the empirically derived basis functions, which individually contribute to the count spectrum; $\boldsymbol{C}$ is the neutron intensity-time profile, which is measured experimentally. Using the method of least-squares, this system of equations can be solved to determine the masses of each initial fissile nuclide present in the sample. The one stipulation is that the delayed neutron intensity curves for each nuclide be unique, as shown in Figure 3.

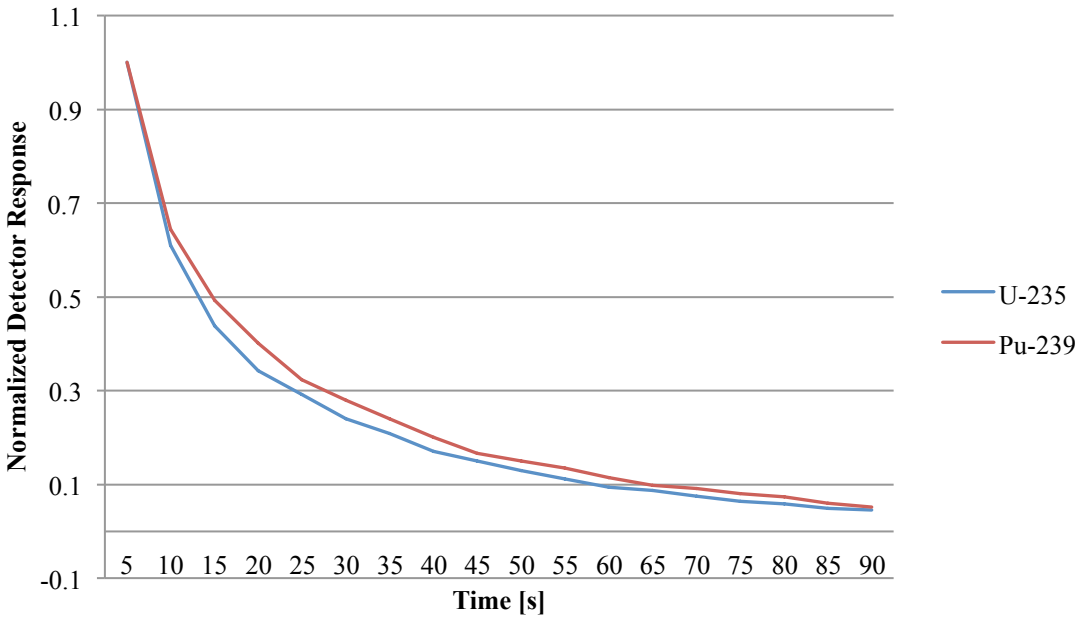

Fig. 3. Neutron decay curves for ^{235}U and ^{239}Pu

Chapter 4

Numerical Analysis

The mathematical formulation of the analysis is rooted in statistical theory that stipulates that given the correct set of circumstances, and observed parameter can be described by a set of definable parameters, or regressors. In the case of this work, the observed parameter is the measured neutron detector response and the regressors are the masses of individual fissile nuclides. The motivation for this chapter is to define the multivariate linear regression model chosen to describe the detector response, and provide justification as to the method used to estimate the parameters of the model.

4.1 Method Overview

The majority of the work performed for this project is the interpretation of the delayed neutron intensity profile of the irradiated samples. The key to success of this work is to determine specific variances that occur in the neutron intensity spectra that can be associated with the presence of a unique fissile nuclide.

The variations in the unique delayed neutron intensity profiles allow for the simultaneous determination of multiple fissile nuclides from a single delayed neutron counting spectrum. To do so, the total neutron intensity profile must undergo deconvolution. This, ultimately, is done by weighting expected neutron intensities for the

constituent fissile nuclides by their masses, the one caveat being that each fissile nuclide must have a unique neutron intensity-time profile.

The analysis begins with approximating the solution to the previously described system of equations using a least squares method. This can be done because the linear combination of neutron intensity count rates represents an *overdetermined* system: it contains more equations than unknown parameters.

Because the total detector response can be taken as η observations made over a period of time so that *c(t)* is a linear combination of ω basis functions, where, again ω corresponds to the number of fissile nuclides present in the sample, as stipulated by Equation 7, the resultant count rate can be expressed in terms of the design matrix, $\boldsymbol{D}$, as

$$\boldsymbol{C}=\boldsymbol{D}.\boldsymbol{m}; \tag{17}$$

where, $\boldsymbol{m}$ is the unknown vector. The design matrix will have the same number of columns as fissile constituents and the number of rows will be equal to the count-time of the system divided by the dwell time of the detector, which was previously defined asη.

Defining the design matrix is a critical step in this analysis. It describes the independent variables of the samples; that is, it defines the shape of the curve based on concentrations of fissile nuclides. The number of independent variables varies, in that if the analysis is only considering delayed neutrons from a single fissile nuclide, there is only a single independent variable. The goal of this work is, partially, to define a multivariable design matrix that will allow for the concurrent quantification of several

fissile components present in a sample. In order to determine the design matrix, standards of single fissile nuclides were created in high concentration and irradiated. This yielded a count rate over a period of time, in this case five minutes, with minimal associated uncertainties. The count rate was then expressed as a matrix, $\boldsymbol{C}$, and imported into MATLAB software. Because only a single fissile component was irradiated on a given standard, $\boldsymbol{m}$ was simply the scalar quantity equal to the mass of the fissile nuclide. $\boldsymbol{P_i}$ was then found simply by dividing the measured $\boldsymbol{C}$ matrix by the known mass, and the basis function for a single fissile component was found in terms of the neutron emission as a function of time and mass [$n.s^{-1}\mu g^{-1}$]. This process was independently repeated for each of the fissile constituents of analytical interest and finally, the design matrix $\boldsymbol{D}$ was defined as the linear combination of the individual basis functions for each fissile constituent.

Once the design matrix was found, unknown samples could be analyzed. These samples were irradiated and counted in an identical fashion. The acquired raw spectrum is then treated as a [η x 1] matrix, defined at $\boldsymbol{C}$ above, where η is the number of time bins sampled and equal to the product of the frequency and the length of sampling time. The system of fissile nuclide masses can be solved as

$$\boldsymbol{m} = (\boldsymbol{D}'\boldsymbol{D})^{-1}\boldsymbol{D}'\boldsymbol{C} \tag{18}$$

Equation 18, however, does not have an exact solution, as $\boldsymbol{D}$ is not a square matrix and does not have an inverse. To this end, the method of least squares was chosen to give an approximate solution for the mass, $\boldsymbol{m}$, vector.

4.2 Least Squares Analysis

The measured delayed neutron emission spectrum of an irradiated sample was described by a multielement regression model. The model defines the neutron spectrum by the contribution of several independent regressor variables. To demonstrate the validity of this method, a model with two independent variables was formulated to describe the delayed neutron activation analysis spectrum of samples containing up to two fissile components. The model has been defined by the relationship

$$\vec{c} = \overrightarrow{P^{o}} + \overrightarrow{P^{U}} m^{U} + \overrightarrow{P^{Pu}} m^{Pu} + \vec{\varepsilon} \tag{19}$$

where the basis function P^{U} describes the change in the neutron spectrum with respect to m^{U}, the mass of ^{235}U present in the sample; likewise, P^{Pu} measures the change in $\vec{c}$ with respect of m^{Pu}.

As it happens, the above expression has no exact solution. Therefore, the spectrum was interpreted using the method of ordinary least squares to determine the fissile masses m^{U} and m^{Pu}. The least squares method determines independent regressors by finding values that force the basis functions to best-fit experimental data. This is done by choosing m^{U} and m^{Pu} that minimize the sum of the squared differences between the measured neutron spectrum and the weighted basis functions at each time step

$$\varepsilon^2 = \sum_{n=1}^{\eta} \left[\overrightarrow{c_n} - \left(\overrightarrow{P^U}_n m^U + \overrightarrow{P^{Pu}}_n m^{Pu} \right) \right]^2 \quad (20)$$

where η is the number of data points in the array $\vec{c}$. The masses m^U and m^{Pu} are determined by finding the critical masses that correspond to minimized sum of the squared errors.

$$\sum \varepsilon_i{}^2 = E(m^U, m^{Pu}) = \sum \left(c_i - P_i^U m^U - P_i^{Pu} m^{Pu} \right)^2 \quad (21)$$

To minimize E(m^U,m^{Pu}), the partial derivatives with respect to the masses is set to zero and solved.

$$\frac{\partial E}{\partial m^U} = 0 = \frac{\partial}{\partial m^U} \left(\sum \left(c_i - P_i^U m^U - P_i^{Pu} m^{Pu} \right)^2 \right) \quad (22)$$

and

$$\frac{\partial E}{\partial m^{Pu}} = 0 = \frac{\partial}{\partial m^{Pu}} \left(\sum \left(c_i - P_i^U m^U - P_i^{Pu} m^{Pu} \right)^2 \right) \quad (23)$$

Evaluating the above expressions yields

$$\frac{\partial E}{\partial m^U} = 0 = 2 \cdot \left(\sum (-P_i^U) \cdot \left(c_i - P_i^U m^U - P_i^{Pu} m^{Pu} \right) \right) \quad (24)$$

and

$$\frac{\partial E}{\partial m^{Pu}} = 0 = 2 \cdot \left(\sum (-P_i^{Pu}) \cdot \left(c_i - P_i^U m^U - P_i^{Pu} m^{Pu} \right) \right) \quad (25)$$

The m^U which satisfies the expression that the partial derivative with respect to m^U equals zero can then be expressed in terms of the measured neutron spectrum and the basis function P^U and P^{Pu}

$$\frac{\partial E}{\partial m^U} = 0 = \sum \left(P_i^U \cdot c_i \right) - m^U \sum \left(P_i^U \right)^2 - m^{Pu} \sum \left(P_i^U \cdot P_i^{Pu} \right) \quad (26)$$

and

$$\frac{\partial E}{\partial m^{Pu}} = 0 = \sum (P_i^{Pu} \cdot c_i) - m^U \sum \left(P_i^U \cdot P_i^{Pu} \right) - m^{Pu} \sum (P_i^{Pu})^2 \quad (27)$$

By simple algebraic manipulations, expressions for the masses can be found in terms of the measured neutron emission profile and basis functions.

$$m^{Pu} = \frac{\sum(P_i^U)^2 \cdot \sum(P_i^{Pu} \cdot c_i) - \sum(P_i^U \cdot c_i) \cdot \sum(P_i^U \cdot P_i^{Pu})}{\sum(P_i^U)^2 \cdot \sum(P_i^{Pu})^2 - (\sum(P_i^U \cdot P_i^{Pu}))^2} \quad (28)$$

$$m^{U} = \frac{\sum(P_i^{Pu})^2 \cdot \sum(P_i^U \cdot c_i) - \sum(P_i^{Pu} \cdot c_i) \cdot \sum(P_i^U \cdot P_i^{Pu})}{\sum(P_i^U)^2 \cdot \sum(P_i^{Pu})^2 - (\sum(P_i^U \cdot P_i^{Pu}))^2} \quad (29)$$

This equation can be generalized for the case where the analyzed sample may contain up to K fissile nuclides

$$\sum_{n=1}^{\eta} \left[\overrightarrow{c_n} - \sum_{i=1}^{K} \left(\overrightarrow{P^i}_n m^i\right)\right]^2 \quad (30)$$

Provided that η>K, the regression model represents an overdetermined system of equations and has a unique solution.

There are a few alternative methods to using an ordinary least squares approach to solve for the nuclide masses. To avoid a tedious and unnecessary discussion on why each of these more advanced methods were not employed, the Gauss-Markov Theorem will instead be used to demonstrate why the ordinary least squares method is the optimal choice for this spectral analysis.

The Gauss-Markov theorem stipulates that under a given set of assumptions, the least squares approximation

$$\widehat{m} = argmin_m \sum \varepsilon^2 \quad (31)$$

is the best unbiased linear estimator, where ε are the residual values between the experimental data and the basis functions weighted by their respective nuclide masses (67) (68). This expression holds true, providing that (69)

1. The parameters, m^i, are linear with respect to C
2. The regressors, P^i, are not collinear
3. $E(\varepsilon_i|m_1, \dots, m_k) = 0$, for all i
4. $V(\varepsilon_i|m_1, \dots, m_k) = \sigma^2$, for all i
5. $cov(\varepsilon_i|m_1, \dots, m_k) = 0$

The Gauss-Markov assumptions hold true for unbiased estimators, so it must first be demonstrated that the model chosen for this work is indeed unbiased. A proof of unbiasedness is as follows. Recall that the multielement regression model of the delayed neutron spectrum

$$\vec{c} = \overrightarrow{P^o} + \overrightarrow{P^U} m^U + \overrightarrow{P^{Pu}} m^{Pu} + \cdots + \overrightarrow{P^N} m^N + \vec{\varepsilon} \tag{32}$$

can be simplified to

$$\vec{c} = \vec{D} \cdot \vec{m} + \vec{\varepsilon} \tag{33}$$

where $\vec{D}$ is the design matrix defined in a previously and vector $\vec{m}$ is an [1xN] array of nuclide masses. To show unbiasedness, it must be demonstrated that the expected value of the nuclide mass array is equal to its true value.

$$E(m) = E\left[(\vec{D}'\vec{D})^{-1}\vec{D}\vec{c}\right] \tag{34}$$

$$E(m) = E\left[\left(\vec{D}'\vec{D}\right)^{-1}\vec{D}(\vec{D} \cdot \vec{m} + \vec{\varepsilon})\right] \tag{35}$$

$$E(m) = E\left[\left(\vec{D}'\vec{D}\right)^{-1}\vec{D}\vec{D}\vec{m} + \left(\vec{D}'\vec{D}\right)^{-1}\vec{D}'\vec{\varepsilon})\right] \tag{36}$$

$$E(m) = E[\vec{m}] + E\left[\left(\vec{D}'\vec{D}\right)^{-1}\vec{D}'\vec{\varepsilon}\right] \tag{37}$$

By definition of an unbiased model

$$E\left[\left(\vec{D}'\vec{D}\right)^{-1}\vec{D}'\vec{\varepsilon}\right] \equiv 0 \tag{38}$$

For this work, the model is unbiased if and only if there are no nonrandom contributing factors to the delayed neutron spectrum except for those which have been modeled by the basis functions. At this point, it can be said with certainty that the parameters P^U and P^{Pu} sufficiently characterized all potential contributors to the spectra. However, as this work progresses and is applied to more complex samples, the above expression becomes increasingly more important; it must be certain that all possible fissile nuclides in the sample be accounted for, otherwise this method will fail.

The first assumption stipulates that the parameters, m^i, are linear with respect to the measured neutron counts. This was experimentally demonstrated by a series of experiments, which quantified the relationship between the detector response and the mass of any nuclide present. For this to be true, the change in detector response with respect to a given basis function must be proportional to the mass of the nuclide present. This is shown by taking the partial derivative of the measured delayed neutron spectrum

$$\vec{c} = \overrightarrow{P^o} + \overrightarrow{P^U}m^U + \overrightarrow{P^{Pu}}m^{Pu} + \cdots + \overrightarrow{P^N}m^N + \vec{\varepsilon} \tag{39}$$

and then can be re-written in terms of the Nth nuclide

$$\vec{c} = \overrightarrow{P^o} + \overrightarrow{P^N}m^N + \sum_{i=1}^{N-1}\overrightarrow{P^i}m^i + \vec{\varepsilon} \tag{40}$$

If $\sum_{i=1}^{N-1} m^i = 0$

$$\frac{\partial \vec{c}}{\partial \overrightarrow{P^N}} = 0 + \frac{\overrightarrow{\partial P^N}}{\partial \overrightarrow{P^N}}m^N + 0 + 0 \tag{41}$$

$$\frac{\partial \vec{c}}{\partial \overrightarrow{P^N}} = m^N \tag{42}$$

To experimentally validate the assumption that the change in detector response is linear with respect to the mass of the nuclide present, a series of standards were analyzed. To confirm the linearity of the model, the relationship between the measured neutron spectrum and the basis function of any nuclide must be linear and equal to the mass of the nuclear present. Figure 4 shows this relationship for ^{235}U; Figure 5 shows this relationship for ^{239}Pu.

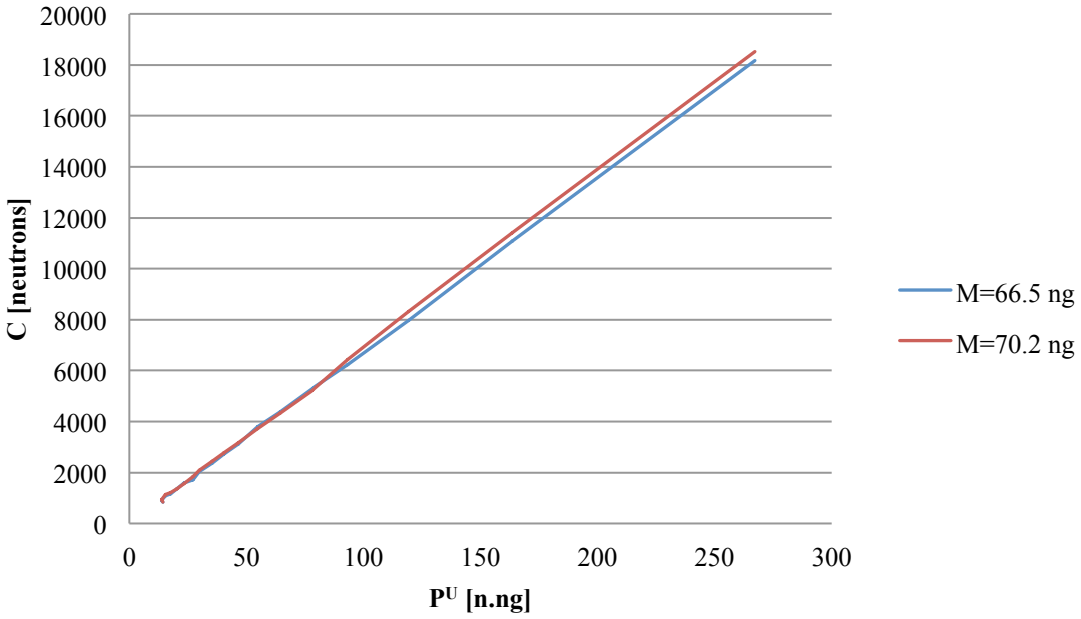

Fig. 4. Linearity of basis function for ^{235}U

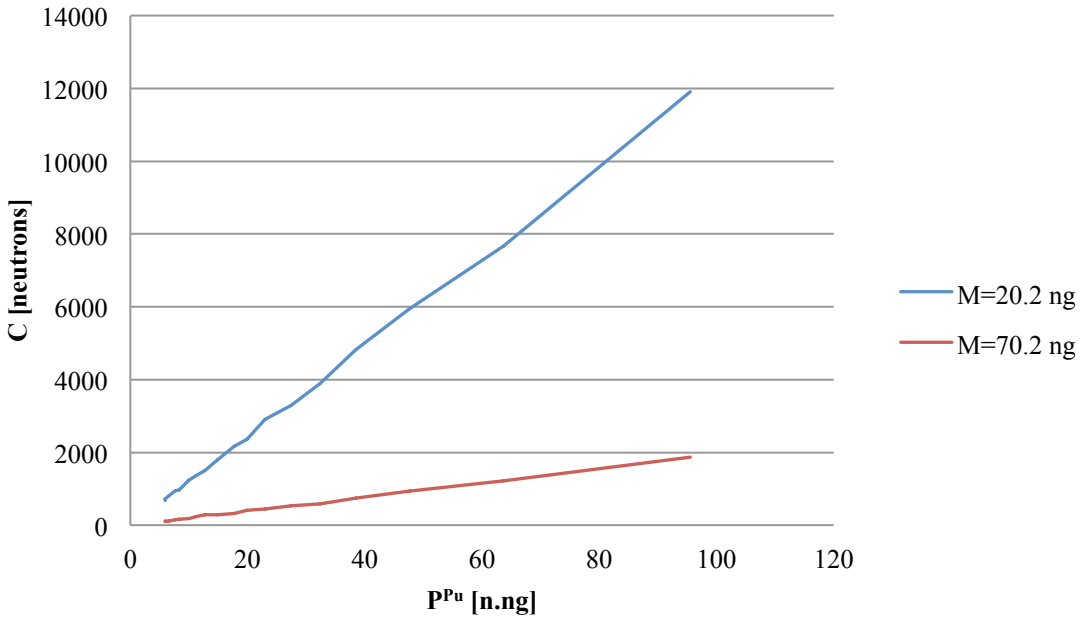

Fig. 5. Linearity of basis function for ^{239}Pu

The above relationships adequately fulfilled the linearity stipulation required for the Gauss-Markov expression to hold true. It then must be shown that the basis functions are not collinear. To show linear independence, it must be true that there is only a single, trivial solution to the expression

$$A \cdot D = 0 \tag{43}$$

where

D is the design matrix, a linear combination of all basis functions

A is a vector of scalar multipliers which satisfies the expression. This was indeed the case for basis functions P^U and P^{Pu}.

Next, it has to be shown that the expected value for the residual error is zero. This does not imply that the error is zero, simply that the error is random and independent with respect to the concentrations of fissile material. Provided that there are no systematic errors and that the model adequately accounts for all fissile nuclides in the sample, this stipulation holds true. To confirm this assumption, the model must meet two criteria: first, that there are no systematic errors, and second that the error did not increase proportionally with increasing sample mass. To demonstrate that this assumption holds true, the relationship between nuclide mass and total sample residual was examined. As can be seen in Figure 6 below, total residual values vary from sample to sample, but there is not an observable correlation between nuclide mass and residual errors.

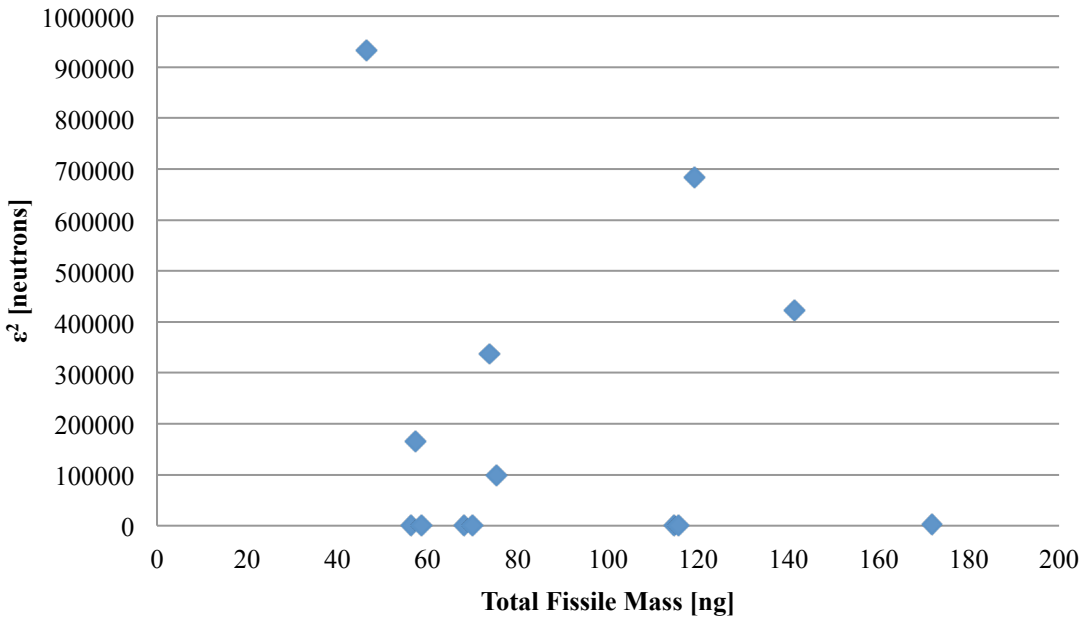

Fig. 6. Uncorrelated relationship between error and sample mass

The nonlinear relationship between the magnitude of the error and the total mass of the fissile material in the sample ensures that Gauss-Markov provision on the expected value of the residual error holds true. Likewise, the variance in the residual error must also be independent of sample mass

The fourth assumption stipulates that all errors have the same variance, which is to say that the model is homoscedastic. Homoscedasticity ensures that the errors have the same uniform variance. If the model is heteroscedastic, the ordinary least squares regression would not provide the best estimate for the nuclide masses. Instead, an appropriately weighted sum of the squares would need to be utilized. Individual values basis vector elements with greater associated errors would be given a smaller weight than basis vector elements with smaller associated errors.

To show that the model is homoscedastic, it must be proved that the associated error does not increase with an increasing independent variable. The null hypothesis is that this holds true, it can be written so that

$$H_o: V(\varepsilon_i|m_1, \dots, m_k) = \sigma^2 \tag{44}$$

Because it has been shown that the expected value of the error is zero, the above expression is equivalent to

$$H_o: E(\varepsilon_i{}^2|m_1, \dots, m_k) = \sigma^2 \tag{45}$$

Therefore, to test whether the model violates the null hypothesis, the data must show that $\varepsilon_i{}^2$ is not related to one or more of the independent variables. This was surveyed by

regressing the squared residuals on the nuclide masses. For a two nuclide-system, the secondary regression becomes

$$\hat{\varepsilon}^2 = \delta_o + \delta^U m^U + \delta^P m^P + v \tag{46}$$

where v is the error term of the errors, which simply has a mean of zero for any nuclide mass. If the independent variables are unrelated to the magnitude of the squared error, it will be shown that

$$\delta^U = \delta^P = 0 \tag{47}$$

The next step, taken from the Breusch-Pagan test for heteroscadasticity, is to find the Lagrange multiplier statistic (70) (71), which is simply proportional to squared residuals between the experimental data and the fitted basis functions

$$LM = nR^2 \tag{48}$$

where n is simply the number of observations and LM is the Lagrange Multiplier statistic. If the null hypothesis holds true, the LM is asymptotically distributed as χ^2. To show the distribution of the Lagrange Multiplier statistic, a known standard was analyzed by a varying number of observations, *n*, and the residual errors were determined for each instance. In other words, an irradiated sample was analyzed multiple times by basis vectors of different sizes. As the number of elements in the basis functions increased, the number of observations increased. The null hypothesis was verified when the relationship between the number of observations and the magnitude of the residuals was found to generally follow a χ^2 distribution. This relationship is plotted below.

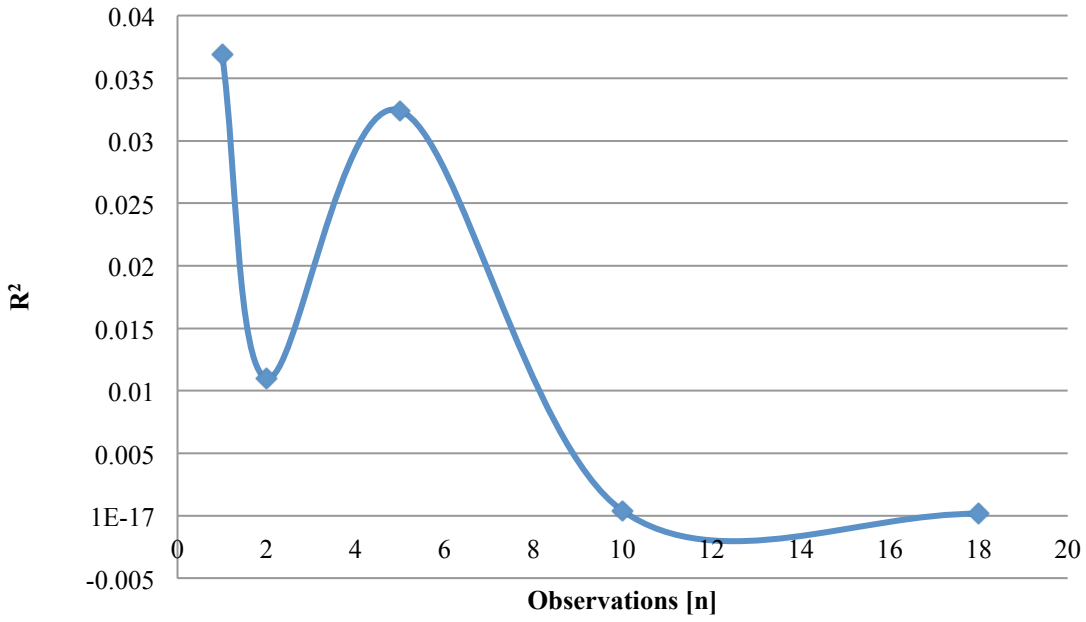

Fig. 7. Relationship between uncertainty and number of observations

The squared residual values of a sample analyzed by basis functions of increasing size showed that as the number of observables in the basis function increases, the magnitude of the residuals between the measured data and the weighted basis functions asymptotically goes to zero. This suggests that the null hypothesis is true, as the results more or less approximated a χ^2 distribution function.

The final stipulation for the Gauss-Markov Theorem to remain valid is that the covariance of the errors due to each nuclide must be zero. This stipulation is also an implied consequence of having shown that *E(ε)=0*, such that

$$cov(\varepsilon, m^U) = E(\varepsilon - E(\varepsilon))(P^U - E(P^U))$$

$$cov(\varepsilon, m^U) = E(\varepsilon(P^U - E(P^U)))$$

$$cov(\varepsilon, m^U) = E(\varepsilon P^U - \varepsilon\, E(P^U))$$

$$cov(\varepsilon, m^U) = E(\varepsilon P^U) - E(\varepsilon)\, E(P^U)$$

$$cov(\varepsilon, m^U) = E(\varepsilon P^U)$$

$$cov(\varepsilon, m^U) = 0$$

This relationship holds true for models in which the number of observations is greater than the number of degrees of freedom in the sample. That is to say, the covariance of the errors is zero if and only if the expected value of the errors is zero and there are more elements in the basis functions (more equations in the set) than there are potential fissile components.

4.3 Overspecifying The Model

As with any statistical model, overspecifying occurs when too many variables are used to describe a regression model. A model can be overspecified in two regards, the first is the inclusion of irrelevant variables, which for this work would mean including basis functions for fissile nuclides that would not be present in the material analyzed. While it has been shown that the linear model will fail if biases due to unaccountable contributors to the spectra are present in the analyte, there are still undesirable consequences to including irrelevant basis functions in the model. The inclusion of too many variables will ultimately effect the variances and consequently the confidence of the masses determined by ordinary least squares.

The second way that a model can be overspecified is to overfit the model. Overfitting occurs when error is modeled into the basis functions. This type of overspecifying is not as innocuous as the inclusion of too many variables. This was avoided in the work by reducing statistical variances in the basis functions caused by detector noise and by excluding basis functions not corresponding to fissile nuclides. One can be tempted to include basis functions for sample background or even the effects of stochastic contributors to the delayed neutron spectrum, such as gamma-ray flux large enough to incur false count rates to the measured neutron spectrum.

The overfitting or overspecifying of any statistical model generally results in poor predictive performance, which in turn leads to poor nuclide estimates in the case of delayed neutron activation analysis. As such, the formulated linear model should include only those basis functions that are neccessary.

4.4 Formulation of Basis Functions

Basis functions numerically describe the delayed neutron emission profile for each fissile nuclide that has been irradiated under a prescribed set of conditions. While it is possible to formulate basis function from the activation parameters, neutron detector efficiency, and known delayed neutron emission data, the technique described here utilizes an empirical method that determined basis functions using isotopically certified reference materials. This was done for several reasons, but mostly because determining a basis function algorithmically introduces significantly more uncertainty. Equation 44 in

fact could be used to describe the delayed neutron emission profile, but the reactor and detector parameters are not well characterized, and the delayed neutron emission data is, at best, an approximation.

$$c(t) = \varepsilon \sum_{i=1}^{N} \frac{m_i N_A}{M} \sigma_f \phi (1 - e^{-\lambda_i t_s}) \sum_{k=1}^{6} \nu_{d_{ki}} \lambda_{ki} e^{-\lambda_{ki} t_c} \quad (49)$$

It was simply easier to produce basis functions, with much greater confidence, using standard reference materials.

The DNAA method outlined by this work was validated by analyzing samples that contained natural uranium, ^{239}Pu, or some mixture thereof. As such, the count rate was described by the expression

$$\overrightarrow{c(t)} = \overrightarrow{P^o} + \overrightarrow{P^U} m^U + \overrightarrow{P^{Pu}} m^{Pu} + \vec{\varepsilon} \quad (50)$$

where $\overrightarrow{P^U}$ and $\overrightarrow{P^{Pu}}$ are the basis functions for ^{235}U and ^{239}Pu, respectively. By preparing a set of standards, which contained only a single fissile nuclide, equation 45 simplifies to either

$$\overrightarrow{c(t)} = \overrightarrow{P^o} + \overrightarrow{P^{Pu}} m^{Pu} + \vec{\varepsilon} \quad (51)$$

$$\overrightarrow{c(t)} = \overrightarrow{P^o} + \overrightarrow{P^U} m^U + \vec{\varepsilon}$$

depending on which nuclide was omitted. To determine the basis function for either nuclide, it becomes a matter of finding the neutron emission rate per unit mass [n.s^{-1}.ng^{-1}]. To solve for the basis function, the assumption was made that the error, ε, had an expected value of zero.

$$E\left(\varepsilon \middle| \overrightarrow{P^U}, \overrightarrow{P^{Pu}}\right) = 0 \quad (52)$$

This expression holds true if the functional relationship between the count rate and the basis functions accurately accounts for the relationship between fissile materials present in the sample and the measured neutrons. In fact, the only reason that the expected value of the error would not be zero is if the model did not account for all fissile material present in the sample; residual analysis of the samples indicated no bias errors and demonstrated that the above relationship holds true. Expressions for the basis functions of ^{235}U and ^{239}Pu can then be written

$$\overrightarrow{P^{Pu}} = \frac{\overrightarrow{c(t)} - \overrightarrow{P^{o}}}{m^{Pu}} \tag{53}$$

$$\overrightarrow{P^{U}} = \frac{\overrightarrow{c(t)} - \overrightarrow{P^{o}}}{m^{U}} \tag{54}$$

In order to mathematically describe the neutron detector response to the βn-decay of ^{235}U, samples containing only uranium were carefully prepared using aliquots of a high-purity natural uranium in a 2% HNO_3 solution with a concentration of 1,000 μg/mL on cotton swipes. Each sample was pipetted and weighed. The cotton swipe was inserted into an irradiation rabbit and allowed to dry in an oven at 85^{o}C for several hours before sealing. ^{235}U samples were made in triplicate and each contained 60 to 70 ng of fissile ^{235}U. The samples were irradiated for 90 seconds and pneumatically returned to the neutron detector array and counted for 90 seconds. As is evident by the following figure, the basis function measurements were repeatable with a two Sigma uncertainty of approximately 3%. While every effort was made to minimize this uncertainty, it was

none the less an unavoidable consequence of using empirically determined basis functions.

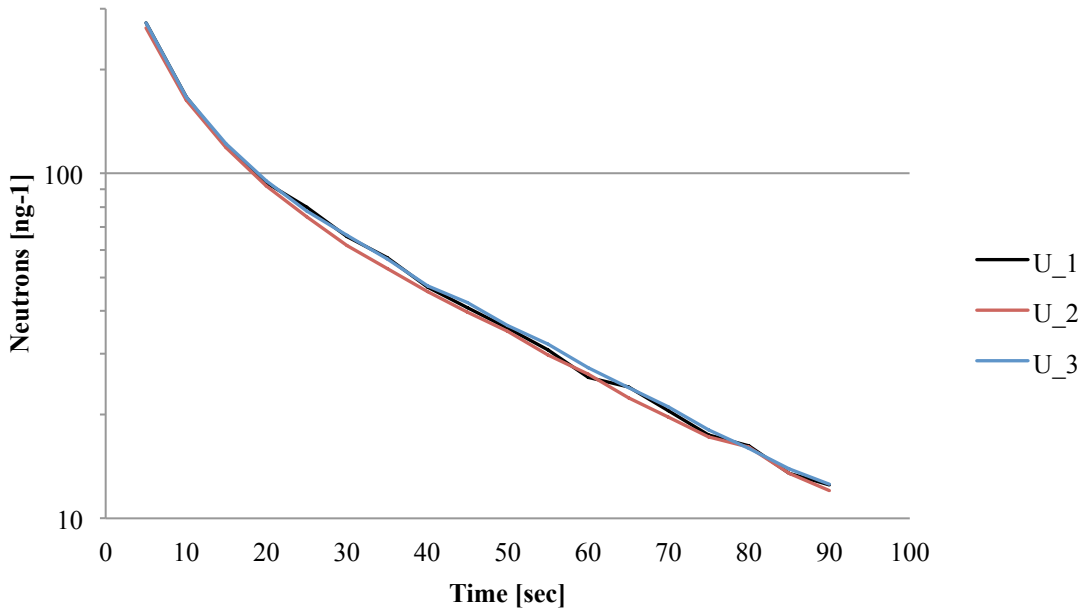

Fig. 8. ^{235}U basis function measurements

This procedure was repeated for samples containing only ^{239}Pu. This of course provided a numerical model for the detector response to the βn-decay of ^{239}Pu. A plutonium isotopic standard solution (CRM 137 from New Brunswick Laboratory) was used as the ^{239}Pu standard for this work. Although the certificate of analysis does show that the solution contained approximately 2 wt% fissile ^{241}Pu, this was ignored. Because of the age of the material and the relatively small amounts of plutonium solution used, any concentration of ^{241}Pu was well below detection limits of this technique and did not affect the delayed neutron spectrum. Samples were prepared in a manner identical to the

procedure outlined above to the preparation of uranium standards; again, efforts were made to ensure that samples were not contaminated with legacy fissile materials from the laboratory, which would falsify the determined basis function. Under identical irradiation and counting parameters, the basis function describing the detector response to the βn-decay of irradiated ^{239}Pu was found. This again was repeated in triplicate; the results of which are plotted below.

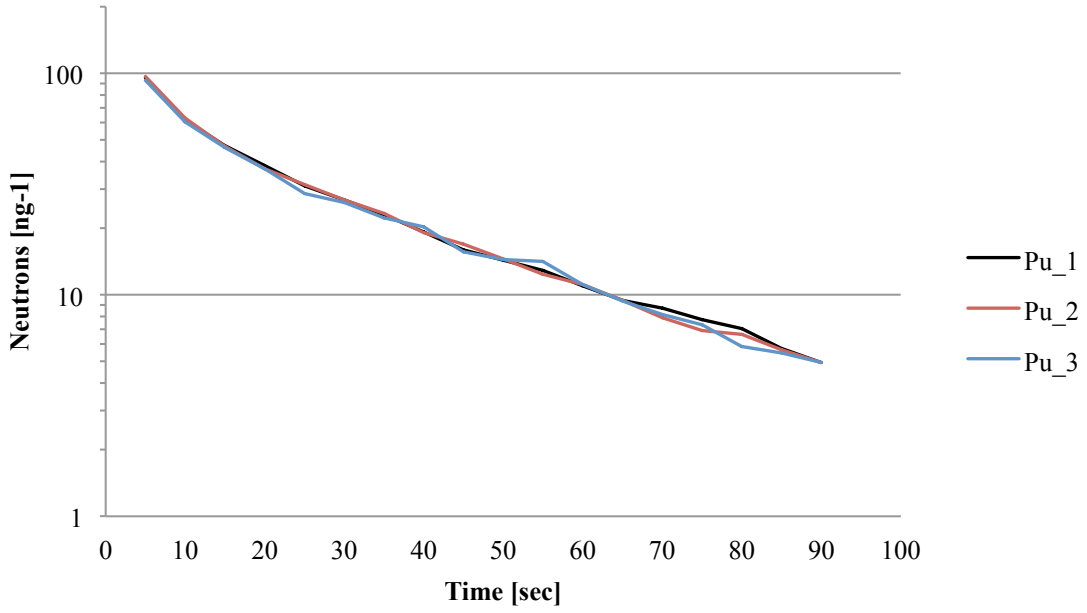

Fig. 9. ^{239}Pu basis function measurements

Again, the results of the plutonium basis function indicated a two Sigma repeatability only to within about 2.5% uncertainty.

Finally, with the introduction of these sources of uncertainty, the model then becomes

$$\overrightarrow{c(t)} = \overrightarrow{P^o} + \overrightarrow{(P^U \pm \sigma^U)} \cdot m^U + \overrightarrow{(P^{Pu} \pm \sigma^U)} \cdot m^{Pu} + \vec{\varepsilon} \quad (55)$$

4.5 Spectral Analysis

The introduction of uncertainty to the individual basis functions poses a unique challenge to the analysis of the delayed neutron spectrum. On one hand, this uncertainty can simply be propagated and taken into account when given the calculated nuclide masses. However, this results in intolerably large uncertainties and errors in the final measurements. It was therefore necessary to better understand the cause of these uncertainties in the basis functions.

The time-dependent delayed neutron emission spectrum of the irradiated standards can be expressed using the activation equation as

$$c(t) = \varepsilon \sum_{i=1}^{N} \frac{m_i N_A}{M} \sigma_f \phi (1 - e^{-\lambda_i t_s}) \sum_{k=1}^{6} \nu_{d_{ki}} \lambda_{ki} e^{-\lambda_{ki}(t_d + t_c)} \quad (56)$$

Nearly every parameter has some uncertainty with it; there is the uncertainty in the mass of the fissile material in the standard and arguably there is at least some variation in the thermal neutron flux. But after careful scrutiny of the technique and the sample preparation methods, it was concluded that the only parameter that could possibly contribute a meaningful uncertainty to the basis function was the decay time of the sample.

Initially, the decay time was considered invariant from sample to sample and equal to the transfer time from the irradiation position to the detector array. However, the current pneumatic transfer system is not capable of indicating the exact transfer time before the sample arrives at its counting position. Intuitively, there are any number of reasons why one sample may return to the detectors a split second faster or slower than another. If a reasonable uncertainty is introduced into the sample decay time, the spontaneous fluctuations in the basis functions are explained.

Because sample decay time cannot be accurately measured, nor can it be predicted which samples will transfer quicker or slower than the standards, it must be assumed that the sample can arrive at any point within the bounds of

$$t_d = \tau_d \pm \Delta t \tag{57}$$

where τ_d is the average decay time, which was found to be roughly 2.1 seconds. Δt bounds the variability in transfer time. The exponential relationship between the neutron spectrum and the decay time of a sample, a small deviation from the expected decay time, greatly changes the neutron emission profile. Setting Δt to 0.1 seconds bounds the basis functions as

$$P_{lower}^{j} \propto \sum_{k=1}^{6} P^{j} e^{-\lambda_{ki} \cdot \Delta t} \tag{58}$$

$$P_{upper}^{j} \propto \sum_{k=1}^{6} P^{j} e^{\lambda_{ki} \cdot \Delta t} \tag{59}$$

Because no mechanism currently exists to accurately measure the sample transfer time and there is no way predict which samples will arrive quicker or slower than the

standards, the assumption must be made that the transfer time can fall anywhere between $\tau_d \pm \Delta t$ with equal probability.

Consequently, when analyzing the measured delayed neutron spectrum, it must take into consideration that the best basis function can be any possible basis function that falls between the upper and lower bounds.

To determine the fissile nuclide masses of an irradiated sample, the delayed neutron spectrum was imported into MATLAB as an array of neutron counts in discrete time bins. The ordinary least squares solution was found for the expression

$$\overrightarrow{c(t)} = \overrightarrow{P^o} + \overrightarrow{P_i^U} m^U + \overrightarrow{P_i^{Pu}} m^{Pu} + \vec{\varepsilon}_i \tag{60}$$

The term $\overrightarrow{P_i^U}$ represents one of the basis functions that falls between the upper and lower bounds of the possible ^{235}U basis functions. Similarly, $\overrightarrow{P_i^{Pu}}$ is one of the basis functions that falls between the upper and lower bounds of the ^{239}Pu basis functions. A script was written in MATLAB, which iteratively found the least squares solutions for the nuclide masses using basis functions that fall within the defined upper and lower bounds. The script than iteratively determined which set of basis functions, $\overrightarrow{P_i^U}$ and $\overrightarrow{P_i^{Pu}}$, correctly accounted for variance in the sample decay time, and consequently, which best predicted the fissile nuclide masses. This was done by evaluating a "goodness of fit" criterion.

The "goodness of fit" parameter was optimized by determining the basis functions that minimized the squared-residuals between the total neutron count over the entire collection period (a scalar quantity, unlike the vector $\overrightarrow{C}$) and the fitted values for m_i^{Pu} and m_i^U. The residuals of the simple regression model can be expressed as

$$\widehat{u_i} = y - (\beta_o + \beta^U m_i^U + \beta^{Pu} m_i^{Pu}) \quad (61)$$

where

$$y = \sum C$$

m_i^U and m_i^{Pu} are the ordinary least squares solution to the expression

$$\overrightarrow{c(t)} = \overrightarrow{P^o} + \overrightarrow{P_i^U} m^U + \overrightarrow{P_i^U} m^{Pu} + \vec{\varepsilon}_i \quad (62)$$

for the i[th] basis functions, and β_o, β^U, and β^{Pu} are scalar coefficients describing the gross neutron counts over the entire counting period and the mass of each fissile nuclide.

The gross neutron counts over the entire counting period was chosen to evaluate calculated nuclide masses because of its much reduced sensitivity to small variances in the sample decay time. The first-order sensitivity index is given by

$$S_i = \frac{P_i}{Var(P)} \quad (63)$$

Figure 10 shows the sensitivity that an uncertainty of 0.1 seconds has on the ^{235}U basis function.

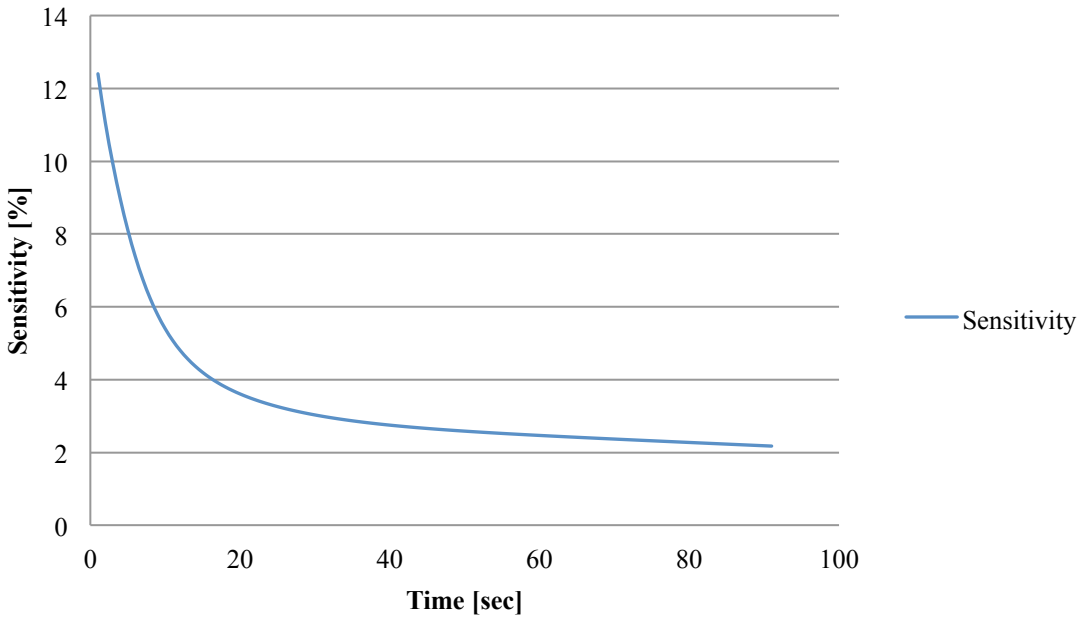

Fig. 10. Δt sensitivity as a function of counting time

As the above figure illustrates, the small variations in decay time become less sensitive with time. The sensitivity of a decay time variance of 0.1 seconds is only approximately 4% for the total neutrons emitted over a 90 second period.

The coefficients β_o, β^U, and β^{Pu} were empirically determined by evaluating the linear relationship between the total neutron detector response and increasing fissile nuclide mass. This relationship was determined by preparing and irradiating two series of reference samples. The first set of standards prepared contained only a variable concentration of ^{239}Pu, m^u=0. This allowed for the change in the total neutron counts, with respect to the concentration of ^{239}Pu, to be described.

$$y = \beta_o + \beta^{Pu} m_i^{Pu} + u \tag{64}$$

The linear relationship between total detector response, measured in total neutrons counted over a 90 second period, and the increasing fissile nuclide mass is shown below in Figure 11. The linearity of the detector response to increasing mass was an important factor when modeling this work with a regression function; had the detector response to increasing mass not been linear, then it would have meant one of two things. The first possibility was that there were unaccounted for contributors to the measured spectrum, in which case the procedure for defining the basis functions would have to be re-evaluated. Or the second possibly would have been that there is a nonlinear detector response to an increasing neutron flux. This latter possibility may come into consideration if some samples contain a large enough mass of fissile material, and detector dead-time and pileup effects cause the response to become nonlinear. However, to this point, experimental data has shown a linear detector response for samples up to 1 microgram of fissile material. This concentration exceeded the typical samples considered for this work; however, the detector response will have to be re-evaluated if this method is applied to samples containing more than 1 microgram of fissile material.

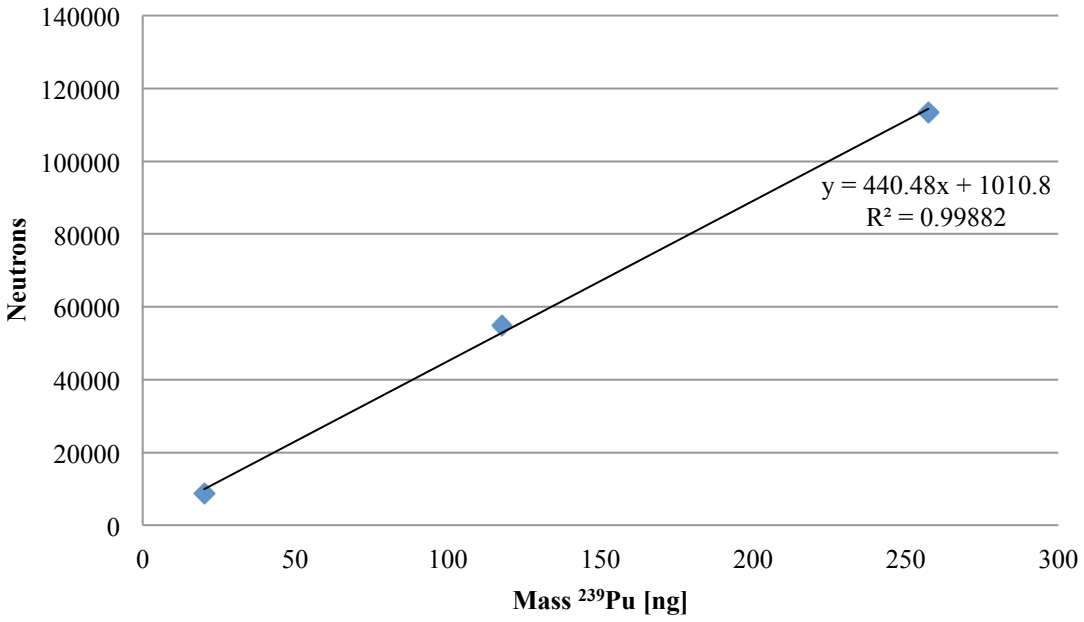

Fig. 11. Linear relationship between ^{239}Pu mass and total neutron counts

The term β^{Pu} was found by determining the best fit linear approximation to the change in total neutrons detected to the change in ^{239}Pu sample mass.

$$\beta^{Pu} = \frac{\Delta y}{\Delta m^{Pu}} \tag{65}$$

The second series of standards contained a fixed concentration of ^{239}Pu (m^{Pu} = 49.15 ng) and a varying concentration of ^{235}U (1.0 ng $\leq$ ^{235}U $\leq$ 50.0 ng). The total neutrons detected over the 90 second period was expressed as

$$y = \beta_o + \beta^U m_i^U + \beta^{Pu} m_i^{Pu} + u \tag{66}$$

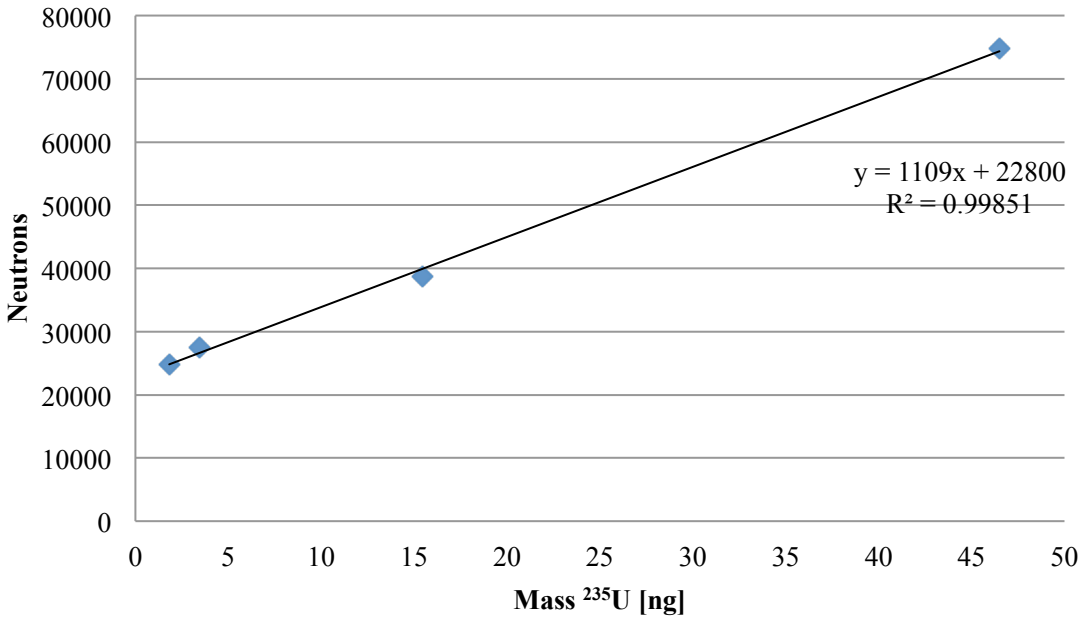

Fig. 12. Linear relationship between ^{235}U and total neutron counts

By determining coefficients β_o, β^U, and β^{Pu}, a second metric was created to evaluate the validity of the masses determined by each of the basis functions.

Chapter 5

System Characterization

Having demonstrated that multiple fissile nuclides can be concurrently determined by measuring the time evolution of the delayed neutron spectrum of an irradiated sample, the method was then carefully scrutinized. This was done for several reasons. First, analyzing the method allowed for a more thorough understanding of the limitations of the technique and by considering these limitations, the applicability of the method could be inferred. Second, by characterizing system specific parameters that effect this method, conclusions were then drawn as to which parameters could be further optimized or improved to better this NAA method.

Both system specific and sample specific characteristics were evaluated. System specific characteristics are those that apply to the method at the High Flux Isotope Reactor and the Neutron Activation Analysis facility at Oak Ridge. The parameters include the neutron flux profile at the irradiation position and specifics regarding the neutron detector array and its associated hardware. Generalized parameters, such as the ideal activation and counting durations were optimized using delayed neutron emission and radioactive decay data, and would not be limited to the irradiations performed at HFIR. Sample specific characteristics are those that apply to the types and quantities of materials best suited for this technique.

5.1 Delayed Neutron Counting System

The Neutron Activation Analysis facility has employed delayed neutron activation analysis for several decades to quantify single fissile isotopes. As such, an existing detector counting array was in place before the start of this project. While some modifications were made, this project worked mostly within the confines of the existing system.

The first modification addressed the fact that delayed neutron counting system initially in place at ORNL was not capable of providing the neutron count rate as a function of time at an adequate sampling frequency. The system was also not capable of digitalizing that the signal so that the data could be interpreted and the neutron spectrum deconvolved.

The system initially utilized an analog ORTEC counter (The ORTEC 974A Quad Counter/Timer). While this counter met the previous analytical needs of the system, which quantified single fissile isotopes, it was inadequate for this work. This counter would only provide an integrated total counts over a preset time period; it would not, however, give the instantaneous delayed neutron count rate, which was required for this work. To rectify this, the hardware was upgraded and a multichannel scaler (MCS) was chosen to replace the analog counter. The ORTEC Easy MCS was chosen out of several commercially available units, due to its computer-interface that allowed for the raw data to easily be imported into MATLAB for signal analysis. A MCS works by recording the number of events in successive time bins. In the case of this work, an event was triggered by the ^{3}He neutron detectors and the time bins were a variables that were

optimized; the greater the sampling frequency, the more susceptible the spectrum was to interferences caused by electronic noise or gamma-radiation. Thus, the detector sampling frequency had to be optimized in order for the delayed neutron signal to be deconvoluted in a manner that the masses of the contributing fissile constituents could be determined.

One of the primary limiting constraints of this work is the sensitivity of the neutron detector system; in order to identify small variances in the time-dependent neutron intensity profile of multiple fissile nuclides, the efficiency of neutron detection must allow for such fidelity. To that end, efforts were made in the preliminary stages of this work to identify optimal detector conditions. The pre-existing delayed neutron counting facility at HFIR utilized 18 gas-filled proportional detectors, arranged in three concentric circles about the irradiated sample. While this configuration had been successfully employed for quite some time, this work provided an opportunity to perform a thorough characterization; it was possible to make adjustments to the system to increase detector efficiency.

The indirect detection of thermal neutrons makes use of one of several mitigating nuclear reactions to compensate for the neutral charge of the incident particles. The neutron activation analysis laboratory at HFIR consists of an annular array of ^{3}He-filled proportional neutron detectors. Helium-3 proportional detectors create a measurable current by using the

$$^{3}He + n \rightarrow \ ^{3}H + \ ^{1}H + 765\ keV \tag{67}$$

reaction to ionize a carrier gas. The (n,p) reaction has a $1/\sqrt{E}$ dependence for low-energy neutrons. Therefore, adequate neutron moderation is necessary to increase the signal output of the detector system. Alternative to ^{3}He gas-filled proportional detectors, boron trifluoride had previously been used in the system. However, BF_3 gas has an increased sensitivity to gamma-rays compared to ^{3}He. While high energy photons would not inherently be expected in the activation products of interest to this work, the background noise had to be minimized and as such, ^{3}He proved to be the optimal detector material.

There is strong correlation between neutron energy and the (n,p) reaction of ^{3}He. Consequently, the key to optimizing the detector system lies in determining how to maximize the thermal neutron flux incident on the detector, while minimizing the total neutron attenuation through the moderator. The optimization was a two-fold approach, determining the ideal position of the detectors and the best neutron moderating material.

To determine the most effective arrangement and position of the gas tubes, Monte Carlo simulations were performed using MCNPX. A simple input deck was comprised of an isotropic neutron source that emitted neutrons with energies consistent with averaged delayed neutron groups. Surface tallies (F2 tallies) were utilized in concentric cylinders about the source. The neutron flux, ϕ, profile as a function of radial distance from the source, r, and energy, e, was obtained. The two parameters of most interest were the thermal neutron flux, ϕ^t, and the unattenuated neutron flux, ϕ_o. The thermal neutron flux was calculated as

$$\phi^t(r) = \int_0^{0.0253\ eV} \phi(E,r)dE \quad (68)$$

where

ϕ(E,r) is the total neutron flux as a function of energy and distance from the source

r is the radial distance from the isotropic neutron emitting source

E is the neutron energy

Also, the attenuated neutron flux was given as

$$\phi(r) = e^{-\mu/\rho \cdot \rho \cdot r} \cdot \int_0^{\infty} \phi(E,r)dE \quad (69)$$

where

μ is the linear attenuation coefficient of neutrons through the moderator, integrated over all delayed neutron energies

ρ is the moderator density

By determining thermal-, and total-, neutron fluxes as a function of radial distance from the source, the detector system was then be optimized to achieve greatest thermal neutron flux, while minimizing attenuation. These calculations were necessary to maximize the (n,p) reaction rate in the proportional detectors, as ^{3}He has a (n,p) cross section of 5328 b at 0.0253 eV. Because delayed neutrons are emitted at energies higher than 0.0253 eV, a moderating material is necessary for optimal detection. Several

different moderating materials were considered, including light water, heavy water, and polyethylene.

5.2 Detector Sampling Frequency

As far as experimental procedures, there were very few parameters that could have been changed. Of course, times of irradiation, decay, and counting were considered, but other than those terms, the NAA procedures allowed for few optimization parameters. The experimental setup, too, was almost entirely unmodifiable, with the one major exception being the detector sampling frequency. The regression model chosen to described the measured neutron spectrum of an irradiated sample collects total neutron emissions over a finite time period. The width of this time bin had significant implications on the resolution capabilities of this method, as the magnitude of the time bins greatly affects the measured signal-to-noise ratio of the total collected spectrum. Assuming that the parametric quantities are sound, the primary contributing factors to the error, ε, can be defined as the detector noise. Random errors arise from a number of sources, but this noise can primarily be attributed to high frequency electromagnetic variances in the detector components.

An idealized expression for the total detector response over a finite time bin can be assumed to have only two components. The first component is simply the signal, which will be defined here as the contribution to the measured spectrum that can be

attributed to the decay of delayed neutron precursors. Using this definition of the term "signal", the noise would simply be equal to the error, as it has been defined previously.

Recall that the expression describing the detector response is not a continuous function but rather a system of linear equations of the form

$$c_k = \beta_o + \sum_{i=1}^{N} \beta_i(t_k \pm \delta) \cdot m_i + \varepsilon \tag{70}$$

The number of equations in the system, η, is equal to

$$\eta = \frac{T}{\delta} \tag{71}$$

where T is the total count time and δ is the detector sampling frequency.

As the collection time bin increases, both the single and noise contributors to the detector response increase, though not at the same rate. Because noise signals at different times are independent events, and therefore uncorrelated, the total noise over a period of $t_i \pm {}^{\delta}/_{2}$ is given as the cross-correlations of independent events and is found as the sum of the squared noise signals, such that

$$Noise = \sqrt{\int_{t_i - {}^{\delta}/_{2}}^{t_i + {}^{\delta}/_{2}} \varepsilon^2} \Rightarrow \sqrt{\delta \varepsilon^2} = \sqrt{\delta}\sqrt{\varepsilon^2} \tag{72}$$

The signal, however, is simply the total signal integrated over the entire time period

$$Signal = \int_{t_i - {}^{\delta}/_{2}}^{t_i + {}^{\delta}/_{2}} \sum P^i m^i \Rightarrow \delta \cdot \sum P^i m^i \tag{73}$$

Consequently, the relationship between the signal-to-noise ratio and the size of the time bins is proportional to the root of the size of the time bin. This relationship stems from

$$\frac{Signal}{Noise} = \frac{\delta \cdot \sum P^i m^i}{\sqrt{\delta}\sqrt{\varepsilon^2}} \propto \frac{\delta}{\sqrt{\delta}} = \sqrt{\delta} \tag{74}$$

As the bin sizes increase, the measured signal fluctuations caused by detector noise decreases in relationship to the total acquired signal.

In order to increase the sensitivity of this technique, the single-to-noise ratio needed to be optimized. The first step was to configure detector components to reduce sensitively to background radiation and false contributors to the neutron spectrum. This was nominally accomplished by operating at a slightly high basis voltage; in all instances to date, collecting enough raw counts from an irradiated sample was not an issue.

The next step then was to optimize a detector sampling frequency that increased the signal-to-noise ratio by decreasing extraneous noise in the spectrum. In essence, because counts are taken at discrete time intervals, this became an exercise in signal summing. The relationship between the measured signal-to-noise ratio with regards to the size of the sampling time bins was measured by measuring the neutron emission of a sealed ^{241}Am(Be) test source. Spectra were acquired for 90 seconds varying the detector sampling frequency from 20 Hz to 0.1 Hz.

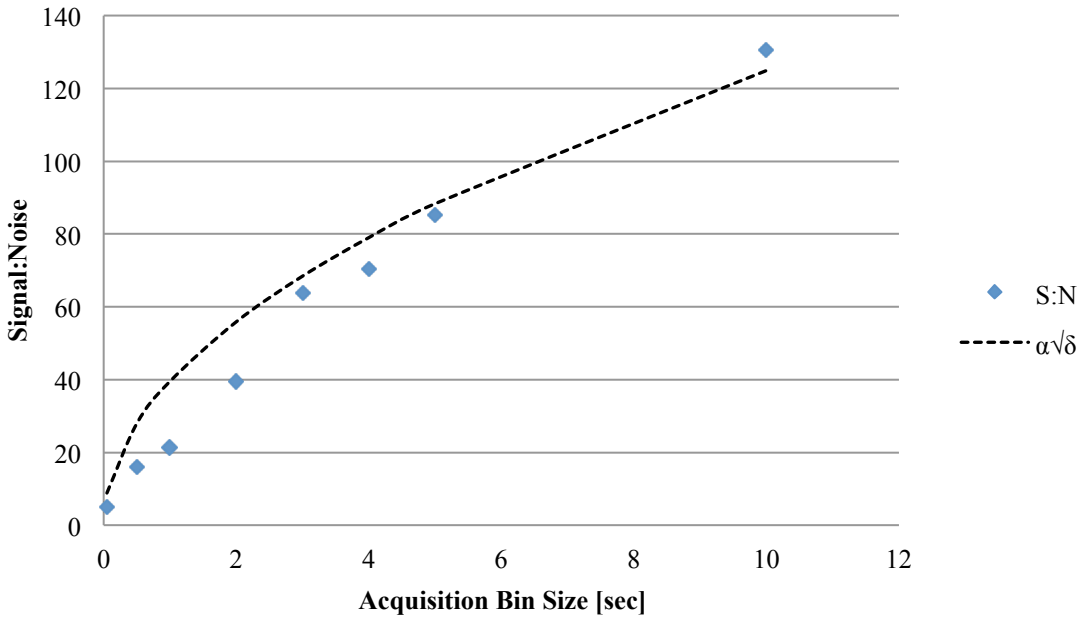

Fig. 13. Signal-to-noise sensitivity to detector bin size

As is evident by Figure 13, above, the measured signal-to-noise ratio generally follows the predicted $\sqrt{\delta}$ relationship (shown as a dashed line in the above figure).

5.3 Neutron Flux Characterization

The other system-specific characteristic of the irradiation is the thermal and fast neutron flux profiles at the irradiation position adjacent to the HFIR core. Based on copious historical measurements, it was expected that there is a significant evolution of the thermal neutron flux over the course of the reactor fuel core lifecycle, which is typically only about 26 days before shutdown and refueling is required. Consequently,

the changing neutron profile translates to variable activation parameters and the need to reformulate basis functions with the changing irradiation dynamics.

Neutron flux measurements were needed to show that despite the evolving flux profile over the course of several weeks, the thermal and fast neutron fluxes remain principally static over short-time periods, on the order of hours so that irradiation and sample measurements can be made in "batches" without continually having to normalize irradiation parameters based on variability of the activating neutron flux. Ideally, if a flux could be considered invariant over a few hours, the basis function would not have to be continually re-evaluated and once they were determined, the functions could be used for a large set of samples. Practically, this translates to more samples processed and analyzed per hour.

In order to demonstrate that the neutron flux profile remains unchanged over the course of an operating day, the fast and thermal neutron fluxes were calculated at several times throughout the day, in intervals of every few hours. High purity Au and Mn foils were irradiated and their respective activities were measured using a HPGe detector. The fast neutron flux was determined using the activation of the $^{197}Au(n,\gamma)^{198}Au$ because of its large resonance absorption cross section of $^{197}Au(n,\gamma)^{198}Au$ at ~4.91 eV. The activation of the Mn foil, $^{55}Mn(n,\gamma)^{56}Mn$, is dominated by the thermal absoption cross-section. The difference in fast and thermal absorption cross sections for each material allowed for the difference in activation product activities to be used to concurrently determine the thermal neutron flux and the fast neutron flux. The thermal:fast ratio could then be inferred from the activation rate of Au to that of Mn (72). Almost as important to

the irradiation parameters as the thermal flux is the assurance that the fast neutron flux remains negligible by comparison so that the fast fissioning of ^{238}U does not contribute to the delayed neutron spectrum during sample analysis, nor do interferences arise due to the $^{17}O(n,p) \rightarrow {}^{17}N + \beta^{-1} \rightarrow {}^{17*}O \rightarrow {}^{16}O+n$, which occurs primarily at high incident neutron energies.

To determine these parameters, expressions for the thermal and fast neutron fluxes were derived from the activation equation

$$A = \sigma^T \phi^T NSDC\theta P_\gamma \xi \quad (75)$$

where

A is the activity at a given energy

σ^T is the total activation cross section, over all energies

ϕ^T is the total neutron flux, over all energies

N is the number of target atoms

S is the saturation factor, $(1-\exp(-\lambda t_i))$, where t_i is the irradiation time

D is the decay factor, $\exp(-\lambda t_d)$, where t_d is the decay time

C is the counting factor, $(1-\exp(-\lambda t_c))$, where t_c is the counting time

P_γ is the emission probability of a photon of a particular energy

ξ is the detector efficiency at a particular photon energy

These total measured activities of ^{198}Au and ^{56}Mn following activation were then used to calculate neutron fluxes. The difference between the total activity of ^{56}Mn and

the activity due to the absorption of fast neutrons was used to derive an expression for the thermal flux

$$\phi^{th} = \frac{A_{Mn}}{N_{Mn}\cdot\sigma_{Mn}^{th}\cdot\left(1-e^{-\lambda_{Mn}t_i}\right)} - \frac{\sigma_{Mn}^{f}}{\sigma_{Mn}^{th}}\cdot\phi^{f} \tag{76}$$

The fast neutron flux was determined from the fast activation of the Au foil; the activity of the Mn foil was needed to correct for the contributions of the thermal activation of Au in the measured activity

$$\phi^{f} = \frac{\frac{A_{Au}}{N_{Au}\cdot\left(1-e^{-\lambda_{Au}t_i}\right)} - \sigma_{Au}^{th}\cdot\frac{A_{Mn}}{N_{Mn}\cdot\sigma_{Mn}^{th}\cdot\left(1-e^{-\lambda_{Mn}t_i}\right)}}{\left(-\frac{\sigma_{Mn}^{f}}{\sigma_{Mn}^{th}}\cdot\sigma_{Au}^{th}\right)+\sigma_{Au}^{f}} \tag{77}$$

The above expressions were used to find the activation parameters over the course of 1 day. Samples were irradiated for 20 seconds and after a variable decay time of a few hours based on maintaining detector dead times <5% (appropriate decay times were corrected for each sample), were counted until appropriate counting statistics were achieved, which took on the order of 15 minutes. It was shown that over the course of an 8 hour operating day, both the thermal and fast neutron fluxes remained unchanged.

5.4 Activation Parameters

Activation parameters were optimized to achieve the greatest detection sensitivity possible. The first parameter considered was the irradiation time. Efforts were made to

keep the total time of analysis as low as possible, so that this protocol could be an effective method of quickly analyzing samples. The general expression for the neutron activation saturation model,

$$S = \left(1 - e^{-\lambda t_i}\right) \tag{78}$$

where S governs the maximum activity immediately following neutron irradiation,

λ is the decay constant of the activation product,

t_i is the time of irradiation.

As $t_i \rightarrow \infty$, S approaches 1, total saturation, asymptotically. Practical constraints are placed on the maximum time of irradiation based on the half-life of the activation product.

Adequate activation saturation, for the purposes of this work, occurred when the saturation factor reached approximately 0.99. Using the above equation and an effective decay constant given by the average averaged decay constants of all delayed neutron precursor nuclides

$$\bar{\lambda} = \frac{\sum_{i=1}^{N} \lambda_i}{N} \tag{79}$$

which was determined using the six-group delayed neutron group data and calculated for both ^{235}U and ^{239}Pu. Using the effective decay constant, an expression for the optimal irradiation time was found

$$t_i = \frac{-\ln (S-1)}{\bar{\lambda}} \tag{80}$$

Figures 14 and 15, below, illustrates that an irradiation time of 90 seconds achieves the desired saturation for both ^{235}U and ^{239}Pu and irradiating for longer periods has an inconsequential increase to the activation saturation.

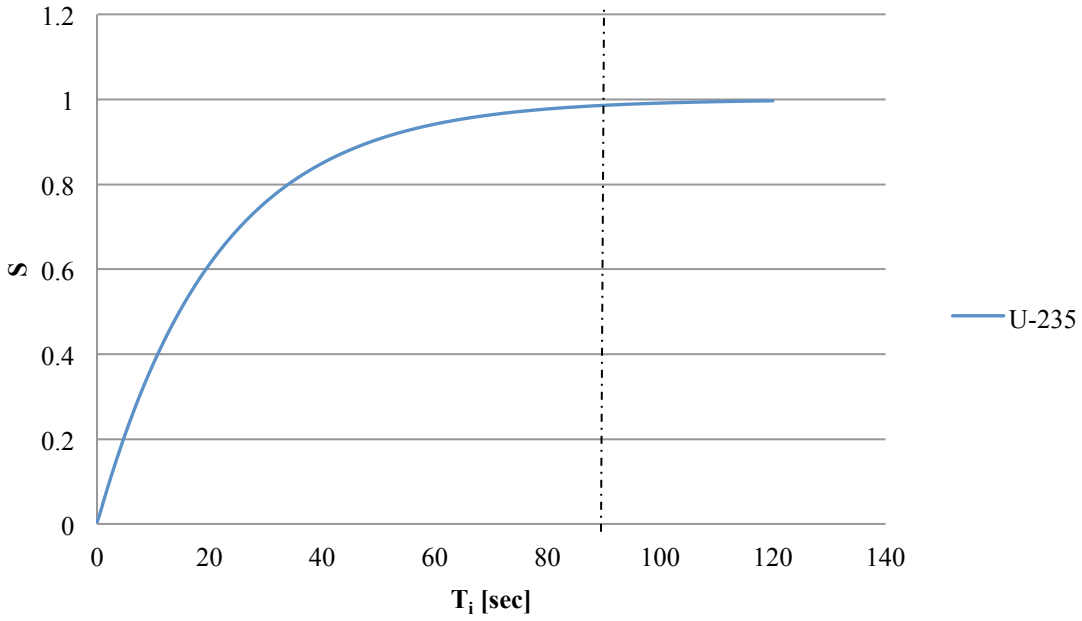

Fig. 14. Saturation as a function of irradiation time for ^{235}U

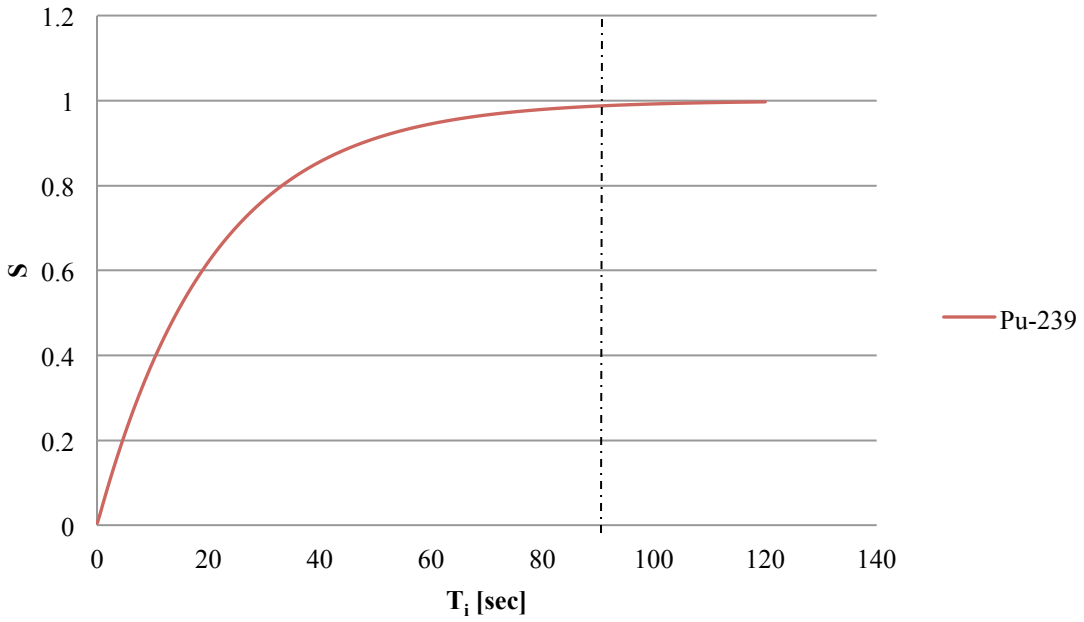

Fig. 15. Saturation as a function of irradiation time for ^{239}Pu

An irradiation time of only 90 seconds was advantageous from a practical standpoint, as it kept the total time of analysis for each sample to a minimum. Early experiments during this project utilized a 180 second irradiation time, giving an effective saturation factor of 0.9998, but this had no observable advantage to the final measurements and only reduced the number of samples that were able to be processed in an hour. For this DNAA method to be practically implemented, the total time of analysis must be kept to a minimum. A 90 second irradiation time was found to be optimal.

If this DNAA method were to be applied at a facility other than HFIR, the irradiation time and other parameters, such as acquisition time optimized here, would be suitable for other neutron sources.

5.5 Acquisition Time

Just as the sample irradiation time was an important parameter optimized, an ideal acquisition, or count time, needed to be found. Because of the negatively exponential relationship between the delayed neutron intensity of an irradiated fissile sample and the length of time after irradiation, there reaches a time when the basis functions of individual nuclides converge to zero. An acquisition time of 90 seconds was chosen for multiple reasons. A practical constraint placed on this method is that it must be capable of analyzing several samples per hour, so a premium was placed on maintaining short collection times. The primary reason for a 90 second count time, however, was that after 90 seconds, the intensity of the delayed neutron emission rate for either ^{235}U or ^{239}Pu is less than 5% of its initial emission rate. Considering again the importance of the signal-to-noise ratio, because the variance in the detector noise is independent of the signal, the noise in the system remains constant throughout the spectrum collection. Consequently, at lower neutron emission rates, the signal becomes increasingly sensitive to the effects of background counts and detector noise. At 90 seconds, an adequate spectrum is recorded and the tail end of the delayed neutron signal is still great enough to not be detrimentally affected by sporadic fluctuations in the measured neutron intensity.

5.6 Lower Limits of Detection

One of the most important metrics when evaluating any analytical technique is the lower limits of detection. Practically, these lower boundaries of detectability govern the technique's applicability to many aspects of nuclear forensic efforts. Offered here is a derivation of the theoretical detection limits for any fissile material, as well as observed detection limits for ^{235}U and ^{239}Pu in mixed uranium-plutonium matrices. A discussion as to the differences between the expected and determined detection limits is given as well.

Theoretical Detection Limits

The classic 1968 paper by Lloyd Currie serves, to this day, as the standard for quantifying detection capabilities of radiochemical analytical methods (73). Currie defined three limiting values: the critical level, L_C, at which point qualitative assertions can be made as to whether or not a signal is detected; the detection limit, L_D, or the minimal concentration needed for quantitative measurements; and the determination limit, L_Q, at which point measurements can be made with a given uncertainty (74). These levels, according to Currie, are expressed as the standard deviation of the background signal, weighted by abscissas of a normal distribution. Expressions for critical levels, detection levels, and determination limits, as a function of counts are given below.

$$L_C = 1.64\sqrt{\mu_B} \tag{81}$$

$$L_D = 2.71 + 3.59\sqrt{\mu_B} \tag{82}$$

$$L_Q = 50\left\{1 + \left[1 + \frac{\mu_B}{25}\right]^{1/2}\right\} \tag{83}$$

Currie defines μ_B as the sum of the limiting mean of the sample blank and the limiting mean of increased background due to interferences. Using the three expressions above, expressions for the critical level and detection limits were derived for this DNAA technique.

In the domain of the detector response, or *count* domain C, μ_B is classically defined as the limiting mean of the blank system response. This definition is a bit of a misnomer in the case of DNAA and should instead be defined as the difference between the gross signal, μ_{B+S}, and the net signal, μ_S. The gross signal is equal to the measured neutron emission, defined previously by the vector $\vec{C}$.

$$\vec{C} = \mu_{B+S} \tag{84}$$

The net signal is then best realized as the signal which can be accounted for by the design matrix, weighted by the masses of the fissile components present in the sample.

$$\mu_S = \sum_{i=1}^{N} \overrightarrow{P^i} m^i \tag{85}$$

Finally, μ_B is then equal to the signal not accounted for by the design matrix. Recalling that the gross signal can be expressed by the multiple regression model,

$$\mu_{B+S} = \vec{C} = \overrightarrow{P^o} + \sum_{i=1}^{N} \overrightarrow{P^i} m^i + \vec{\varepsilon} \tag{86}$$

Then μ_B can be expressed by the sum of the sample blank plus the error

$$\mu_B = \overrightarrow{P^o} + \vec{\varepsilon} \tag{87}$$

μ_B, which is perhaps most intuitively realized as the signal unaccounted for, can be calculated as the magnitude of the difference between the total detector response and the signal attributed by the fissile material in the sample,

$$\mu_B = \left|\vec{C} - \sum_{i=1}^{N} \vec{\beta}_i m_i\right| \tag{88}$$

By the transitive property, this value of μ_B directly corresponds to what is often simply referred to as the "mean background signal" and can therefore be used to find the critical, detection, and determination limits using equations 81, 82, and 83, respectively. These expressions can be redefined as

$$L_C = 1.64\sqrt{\left|\vec{C} - \sum_{i=1}^{N} \vec{\beta}_i m_i\right|} \tag{89}$$

$$L_D = 2.71 + 3.59\sqrt{\left|\vec{C} - \sum_{i=1}^{N} \vec{\beta}_i m_i\right|} \tag{90}$$

$$L_Q = 50\left\{1 + \left[1 + \frac{\left|\vec{C} - \sum_{i=1}^{N} \vec{\beta}_i m_i\right|}{25}\right]^{1/2}\right\} \tag{91}$$

In order to get meaningful detection limit values, L_C, L_D,and L_Q, need to be transformed into the mass domain by letting by f: C→m by $f(\mu) =: \frac{\mu}{\vec{\beta}_i}$, where $\vec{\beta}_i$ is the basis function of any fissile nuclide, *i*.

Finally, expressions for the lower limits of detection in the domain m can be expressed

$$L_C = \frac{1.64\sqrt{\left|\vec{C} - \sum_{i=1}^{N} \vec{\beta}_i m_i\right|}}{\vec{\beta}_i} \tag{94}$$

$$L_D = \frac{2.71 + 3.59\sqrt{\left|\vec{C} - \sum_{i=1}^{N} \vec{\beta}_i m_i\right|}}{\vec{\beta}_i} \tag{95}$$

$$L_Q = \frac{50\left\{1+\left[1+\frac{\left|\vec{C}-\sum_{i=1}^{N}\vec{\beta}_i m_i\right|}{25}\right]^{1/2}\right\}}{\overrightarrow{\beta_i}} \tag{96}$$

An interesting, although not unexpected, consequence that emerges from the above expression is that as the number of basis functions increases, lower bounds of detection also increase. This is due to the introduction of uncertainty and increasing residual values in each basis function. This becomes meaningful as this method is applied to even more complex materials, which could potentially include three or more fissile nuclides.

Measured Detection Limits

Detection limits for ^{235}U and ^{239}Pu in a binary mixture of ^{239}Pu and ^{235}U were determined using the expressions derived previously. 19 mixed samples were irradiated, counted, and critical, detection, and determination limits were calculated for each sample. The results of which are plotted in Figs. 16 and 17 for ^{239}Pu and ^{235}U, respectively.

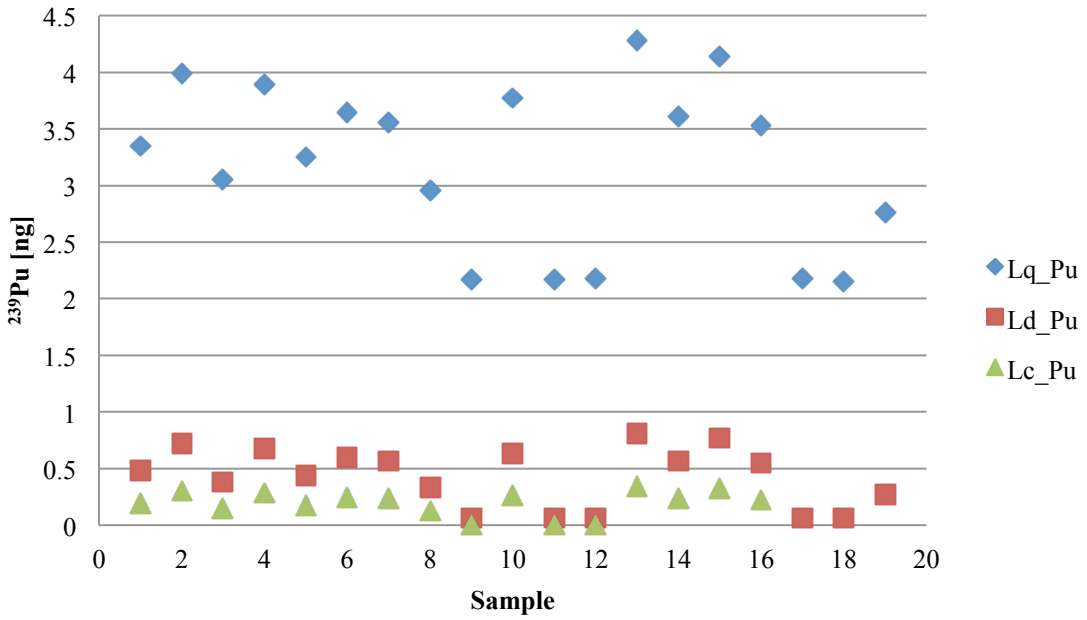

Figure 16. Detection, Critical, and Determination Limits of ^{239}Pu

Figure 16 shows the lower limits of detection and quantification for ^{239}Pu in samples containing a binary mixture of natural uranium and fissile plutonium. The limits were calculated using the total residual values of a set of analyzed reference standards.

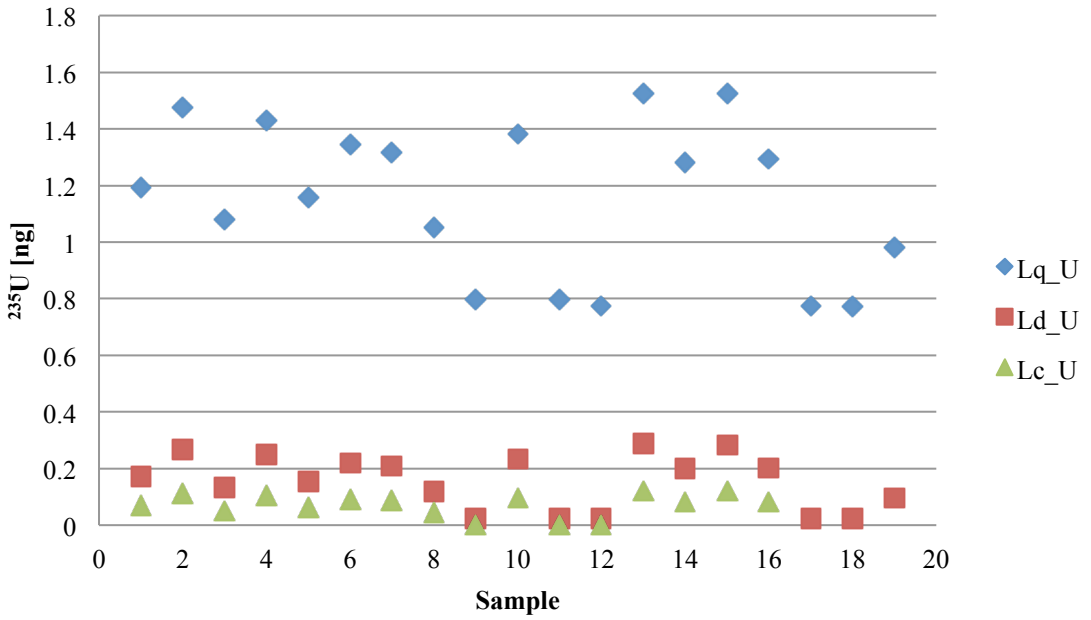

Fig. 17. Detection, Critical, and Determination Limits of ^{235}U

Determination limits were consistently on the order of 1-2 nanograms of ^{235}U and twice that for ^{239}Pu. These values are several orders of magnitude greater than detection limits typically offered by advanced mass spectrometry techniques. The difference between the limits for ^{235}U and ^{239}Pu correspond with the number of delayed neutrons emitted per nuclide; ^{235}U emits, on average, about 2.5 times as many delayed neutrons per fission event than ^{239}Pu. Because fewer neutrons are emitted per nanogram of material present, a greater concentration of ^{239}Pu than ^{235}U is needed to achieve minimum detection limits.

Chapter 6

Error and Uncertainty

Once a method was determined, the most important metric evaluated was the uncertainty of the associated with the determined results. A thorough understanding of the major contributors to the uncertainty of the measurements was vital to the analytical technique. However, an important distinction must be made between errors and measurements uncertainties. As will be discussed in greater detail, errors arise in the form of unaccountable contributors to the measured spectrum. The uncertainty in measurements stems from a variety of factors, but as will be shown, the uncertainty of the determined nuclide masses is dominated by only a few parameters.

6.1 Errors

Recall that a multi-element regression model is used to describe the measured delayed neutron emission spectrum of the form

$$\overrightarrow{c(t)} = \overrightarrow{P^o} + \overrightarrow{P^U} m^U + \overrightarrow{P^{Pu}} m^{Pu} + \vec{\varepsilon} \quad (95)$$

The errors, $\vec{\varepsilon}$, arise from the counts that cannot be described as part of the background, $\overrightarrow{P^o}$, or the parameters described by either the uranium or plutonium basis functions. In order to minimize the background, detector parameters were optimized; in order to

minimize the error such that the expected value of $\vec{\varepsilon}$ was zero, all contributors and potential contributors to the spectrum were defined by a well categorized design matrix.

Adequately defining the background spectrum and minimizing it is one of the single most important ways to minimize the error. Another way to minimize the error is to optimize detector parameters and adequately define the basis functions. To optimize the detector system parameters, in an effort to minimize background signals to the spectrum, it was necessary to be mindful of the causes of an increased neutron background spectrum. The minor contributors to the signal can be secondary neutron radiation from cosmic ion radiation interactions or even terrestrial natural neutron irradiation (75) and are accounted for by the term $\overrightarrow{Po}$. Detector response due to an induced γ-flux must also be taken into consideration.

There are several ways to account for the effects of γ radiation on the detector array. The first is to describe the effects of the short and long-lived radionuclides that could potentially be present. Practically speaking, this was avoided for two reasons. First, the design matrix would have become overly complicated if basis functions were defined for the detector response to high and low energy, short and long-lived γ emitting nuclides. The second motivation for not characterizing the spectrum in this way was that findings have consistently shown that using BF_3 neutron detectors, as were used for this work, have a negligible response to γ radiation (76) (77) and therefore the characterization is not needed. The detectors were optimized not to maximize the neutron signal, but to minimize noise; high detector bias voltages were primarily responsible for minimizing any detector response to an induced γ field.

Once $\overrightarrow{Po}$ is minimized, $\vec{\varepsilon}$ can be evaluated. The condition that must be met is that

$$\mathrm{E}(\varepsilon_i | m^U, m^{Pu}) = 0 \tag{96}$$

Conceptually, this stipulation says that the error must be due to random fluctuations and not due to an unaccounted contributing factor to the measured delayed neutron spectrum. By minimizing the background counts, many would-be contributors (such as natural background radiation) are not recorded by the detector array and are therefore not a significant source of error.

If nonrandom or systematic contributors to the delayed neutron spectrum were present but otherwise unaccounted for, they would be qualitatively observed in the residual spectrum. The residual spectrum is simply the difference between the measured spectrum and the neutrons accounted for by the weighted basis functions. This is given by the expression:

$$\vec{R} = \vec{D} \cdot m - \vec{C} \tag{97}$$

By evaluating the residuals for spectra containing ^{239}Pu, ^{235}U or a mixture of the two materials, it was confirmed that the design matrix was adequate and that the errors were random and minimal. However, there were still errors, and these errors were taken into consideration when calculating the uncertainty of the determined nuclide masses.

What will hereafter be referred to as the spectral *fit-factor* is a quantity that describes the difference between the measured neutron emission profile and the design matrix, weighted by the calculated nuclide masses. The fit-factor serves as a numerical representation of the error that arises from fitting explanatory functions to a measured neutron emission profile.

The fit-factor parameter is an expression of the total measured neutrons which were not accounted for by the basis functions. The error due to the fit-factor for the N^{th} fissile nuclide is expressed as

$$\sigma_{ff}^{N} = \frac{\Sigma|c_i - \Sigma P_i^n m^n|}{\beta^N} \quad (98)$$

The fit factor expression was used to determine the mass uncertainty for each nuclide due to poor fitting statistics.

By definition, errors are quantified differences between the value of a measurement and an individual result (78). These errors between the predicted spectrum and the measured spectrum are transcribed into a measurement uncertainty by the above equation, which weights the difference in counts by the scalar coefficients describing the gross neutron counts over the entire counting period and the mass of each fissile nuclide.

6.2 Uncertainty

Uncertainties, fundamentally different from errors, arise from measurements made and represent a dispersion of possible values the quantified value might reasonably take. It is important that all uncertainties that contribute to the final uncertainty of the determined nuclide masses are well understood; while uncertainties certainly cannot be eliminated from any analytical method, their reduction and minimization greatly enhance the precision of the method. The uncertainties that contribute to the range of possible values that the final nuclide masses may take stem from numerous sources, all of which

can be classified as belonging to either uncertainties from the preparation of the standards set or uncertainties in the irradiation parameters.

The preparation of the standards set, which was needed in order to empirically model the fissile nuclide basis functions, introduced much of the dominating total uncertainty. The major contributors to this uncertainty are caused by instrumentation and reagent purity. Minor contributors, such as those caused by measurement conditions (the temperature of the room during sample preparation), sample blanks and background, and operator effects were considered, though not propagated to the total measurement uncertainty of the nuclide masses. These minor contributors were accounted for and corrected ad hoc, by accounting for small variations of reference material density due to temperature differences, making repeated measurements of sample blanks to ensure that natural fissile material in the cotton was below detectable limits, and by two-person verification of irradiation processes to ensure operator effects had negligible bearing on measurements. Beginning with the reference materials themselves, the certified elemental composition of the standards as well as their isotopic composition both limited the precision of the final analysis. These uncertainty terms will be defined as

σ_E and σ_I

where the subscripts E and I represent the uncertainties due to the elemental concentration of the reference standard and the uncertainty of its isotopic composition, respectively. In preparation of the standards, where cotton swipes were spiked with concentrations of fissile reference material, uncertainty was introduced by way of measurement uncertainty of the balance. The materials themselves were aqueous, and

were pipetted onto the cotton substrates, but the sample masses were also measured, as well as volumes, for more precise measurements. The uncertainty of the balance used at the Neutron Activation Analysis Lab in preparation of the standards is defined by the term

$$\sigma_M$$

The remaining sources of uncertainty come from uncertainties in the activation, decay, and counting of the standards and unknown samples. The neutron activation of the sample introduces many sources of uncertainty, though the total uncertainty of the measurements is dominated by only a few.

The irradiation of the samples themselves introduced many minor contributors of uncertainty. The one parameter that was shown to evolve over the lifecycle of the reactor core is the thermal neutron flux. Small permutations in thermal neutron flux alter the activation parameters from sample to sample. After conducting flux measurements at various times during the reactor core cycle, it was found that on time frames that are short compared to the life cycle of the core, these flux variations do not add a measurable uncertainty to the nuclide measurements. A characterization of the flux is offered in Chapter 5; however, there is only a negligible change in the neutron flux over a period of a few hours. As long as samples are irradiated and counted in "batches", this stipulation holds true. However, basis functions will have to be reconfigured if measurements are repeated at a later time in the reactor lifecycle. Other uncertainties that arise during the irradiation period of the sample analysis have negligible effects on the total measurement uncertainty. Measurement uncertainties associated with other terms of the activation

equation, such as uncertainties in the fission cross sections and decay constants are well below the analytical capabilities of this method and were therefore omitted from the final propagated measurement uncertainty.

As has already been discussed, the uncertainties that arise due to fluctuations in the sample decay time have been addressed as a separate issue. A decay time uncertainty of $\Delta t = 0.1$ seconds was assumed in the numerical evaluation of the delayed neutron spectrum and masses were iteratively solved using a direct enumeration method. The numerical evaluation solved for the nuclide masses using basis functions that fell within the upper and lower bounds of the range of basis functions by solving for discrete basis functions at decay time variation of <0.005 seconds. Consequently, an effective decay time uncertainty of this magnitude is of negligible consequence to the total measurement uncertainty and was omitted from propagation.

Uncertainties, which arise due to counting parameters, were considered and individually evaluated. Geometric effects on the total counting efficiency were briefly considered during the initial stages of this investigation. However, due to the physical constraints of the irradiation vessel and the arrival position in the neutron detector array, there was only a small variability of sample geometry. Further, a literature search confirmed the experimental observations that geometric effects account for only a small fraction of the total combined uncertainty. A 2008 paper by Greenberg at the National Institute of Standards and Technology suggested an uncertainty of $< 0.01\%$ for geometric counting effects, for small samples of similar shape. Further, the same paper also confirms the observations that small variations of sample placement within the irradiation

rabbit have a negligible effect on the neutron fluence exposure (79). This holds true for samples of the same size; if this method were to be applied to other samples, this parameter will need to be revisited, but for the purposes of irradiating and counting cotton swipe materials, small variations in sample geometry did not cause an observable variation in the delayed neutron emission spectrum.

To quantify the measurement uncertainty of the calculated masses, the combined standard uncertainty is found by the square root of the sum of the squared uncertainty components

$$u = \sqrt{\sum \sigma_i^2} \tag{99}$$

The expanded uncertainty, which weights the standard uncertainty by a coverage factor chosen by a desired confidence level, is given by

$$U = k \cdot \sqrt{\sum \sigma_i^2} \tag{100}$$

Uncertainties presented for this work were determined by finding the standard uncertainty of the major contributing factors to the total measurement uncertainty at a confidence interval of 95%. These uncertainties were found by the expression

$$U = 2 \cdot \sqrt{\sigma_M^2 + \sigma_E^2 + \sigma_I^2 + \sigma_{ff}^2} \tag{101}$$

The above expression defines the interval about the resultant nuclide mass

$$m^i - U_{95} \leq M^i \leq m^i + U_{95} \tag{102}$$

Where m^i is the resultant mass found by the analytical method and M^i is the true value of the mass of the i^{th} nuclide present in the sample.

6.3 Conclusions

The range and type of applications this application of delayed neutron activation analysis has is ultimately dictated by these final uncertainties. The sensitivity of mass measurements is one of the primary factors when evaluating this technique and choosing it above other, more sensitive, destructive analytical methods.

The dominating contributors to the total uncertainty of the nuclide measurements are those associated with fitting errors and the preparation of the standards. It is feasible to lower the magnitude of each of these parameters, especially the later, with different, more resolute reference materials. The more precise the standards used to characterize the delayed neutron emission profiles for each nuclide, the better the analytical capability of this method will be as a whole. However, under the constraints of this project and the materials at hand, these uncertainties were at a minimum.

Chapter 7

Validation Experiment

To test and validate this delayed neutron activation analysis technique, a final experiment was conducted. A series of seventeen samples were prepared on cotton swipes and measured. The purpose of this experiment was threefold: to substantiate the claim that this method is capable of accurately determining uranium in the presence of plutonium, which is often experimentally challenging using even the most advanced mass spectrometric techniques. Similarly, this experiment sought to confirm that plutonium measurements could be made in mixed samples without chemical separation. Finally, the experiments were performed to validate this method and confirm the hypothesized capability of nondestructively concurrently determining multiple fissile nuclides.

The analytical procedure can easily be discretized into two major tasks. The first was the irradiation of samples made in-house to experimentally validate the mathematical formulation described previously. The second task was the data analysis and the creation of an analytical protocol for the simultaneous quantification of multiple fissile constituents using a single delayed neutron intensity profile.

While delayed neutron counting has been utilized as a method of quantifying fissile material at HFIR for many years, this work does so in a much different fashion (80) (81), and as such, multiple nuclides can be quantified concurrently. Up to this point, the counting system at HFIR has primarily been utilized for single-isotope quantification

by comparative method, where the integrated count rate over a prescribed period of time is determined for a known standard and an unknown sample. The ratio of the total counts is equal to the ratio of the masses (82). This method has been used exhaustively by numerous facilities for similar analysis; however, the presence of multiple fissile components cannot be identified using this method. Further, if a sample were to contain multiple fissile components, the results of such analysis would be erroneous.

7.1 Procedure

Samples were prepared parallel to the procedure outlined for the preparation of the standards used to characterize the system. Isotopically certificated reference materials were pipetted and massed to ensure accuracy of the samples onto cotton substrates similar to the TexWipe materials used by the IAEA for environmental swipe sampling. The substrates were then dried and inserted into irradiation rabbits. The rabbits were assigned random numerical identifiers. While this was not a blind study in the truest sense, efforts were made to ensure that the nuclide concentrations were not obviously known during analysis.

The following protocol, which had been optimized by experiments prior, was used to analyze the sample series.

1. Background detector measurements were taken. This involved taking gross neutron counts over 400 second periods to ensure low detector background and noise. 90-second time resolved count measurements were also made to ensure that the background was both minimal and linear.

Background measurements on the order of less than 1 count per second ensure that the system was operating properly.

2. Next, "sample blanks" were irradiated and counted. The sample blanks consisted of cotton substrates with no fissile material added. The blank samples were irradiated and counted for 90 seconds. This was to provide an accurate P^o measurement and to ensure that any natural background uranium present in the cotton material was below detection capabilities.
3. Reference standards were then analyzed. Due to variability in neutron flux over the course of the reactor cycle, basis functions were re-determined prior to each batch of samples. Reference standards were prepared and analyzed in triplicate.
4. Samples were then irradiated. The ideal irradiation procedures were found to be: irradiate for 90 seconds; decay for roughly 2 seconds; and count for 90 seconds. Time resolved neutron count profiles were recorded and saved as an ACSII file that could be imported into MATLAB and Excel.

Following counting, the samples were returned to a lead dump-tank for decay for several hours and the procedure could be repeated for subsequent samples. On average 12-15 samples were processed per hour. The spectra were then imported into MATLAB for analysis.

Two scripts were written in MATLAB. The first script used the neutron emission profiles of the irradiated standards to determine the basis functions. By preparing

multiple standards, basis functions were averaged and upper and lower bounds using a decay time variance of 0.1 seconds were determined for ^{235}U and ^{239}Pu.

The second script took the spectral data and iteratively solved for nuclide masses using the range of possible basis functions and determined the best solution based on the minimal variance of the gross neutron count. The script also found critical detection and determination limits based on the residual values for each sample.

7.2 Results

The results of the final experiment showed promise for the described technique. As the tabulated results show, this method is unequivocally capable of measuring multiple fissile nuclides, simultaneously, without destructive chemical sample preparation. Further, this technique successfully measured uranium concentrations in mixed actinide samples; this often causes analytical difficulties using advanced mass spectrometric techniques because of the mass-interferences that often arise due to the formation of hydrides.

Table 3 gives the final measured uranium and plutonium masses determined by this method. Uncertainties are provided and have been calculated using the method described in Chapter 5. The predicted nuclide masses given are the certified reference values; uncertainties arise from the cited uncertainty values provided by the certificate of analysis and measuring uncertainties in sample preparation.

Also tabulated are the detection, critical, and determination limits, as calculated by the method previously described, for each sample. The uncertainties given for each results were calculated using the expression derived in the previous chapter, with a convergence factor of 2, which approximately corresponds to the 95% confidence level of the measurements. There were a few samples with higher uncertainties than other measurements; these uncertainties were driven by poor fitting statistics.

Table 3. Results of validation experiment

	Certified Values		Measured Values	
Sample	^{235}U [ng]	^{239}Pu [ng]	^{235}U [ng]	^{239}Pu [ng]
1	1.821 ± 0.210	49.153 ± 0.712	< L_Q	56.09 ± 1.43
2	46.709 ± 0.215	32.294 ± 0.712	47.33 ± 1.11	32.85 ± 2.99
3	3.431 ± 0.210	49.153 ± 0.712	2.46 ± 0.42	56.04 ± 1.45
4	46.429 ± 0.215	73.611 ± 0.713	46.19 ± 1.55	73.31 ± 4.01
5	15.476 ± 0.211	49.153 ± 0.712	19.02 ± 0.84	39.81 ± 2.99
6	46.289 ± 0.215	105.905 ± 0.713	41.93 ± 1.25	109.09 ± 3.27
7	24.720 ± 0.211	51.528 ± 0.713	22.95 ± 0.73	55.99 ± 2.01
8	46.499 ± 0.215	49.865 ± 0.713	47.11 ± 1.78	50.52 ± 4.61
9	0 ± 0	123.951 ± 0.713	< L_Q	129.18 ± 1.42
10	66.528 ± 0.220	0 ± 0	68.31 ± 0.44	< L_Q
11	0 ± 0	125.376 ± 0.713	< L_Q	126.28 ± 1.43
12	0 ± 0	117.778 ± 0.713	< L_Q	124.60 ± 1.45
13	105.814 ± 0.235	221.783 ± 0.715	110.07 ± 3.48	203.76 ± 8.82
14	105.324 ± 0.235	116.353 ± 0.713	98.78 ± 3.47	126.74 ± 8.82
15	123.251 ± 0.235	116.828 ± 0.713	124.14 ± 4.25	110.89 ± 10.75
16	70.799 ± 0.222	47.491 ± 0.712	67.07 ± 2.17	54.57 ± 5.55
17	141.739 ± 0.253	23.983 ± 0.712	136.03 ± 0.57	25.12 ± 1.58
18	0 ± 0	20.184 ± 0.712	< L_Q	19.63 ± 1.42

There are a few key observations that can be made in light of the results tabulated above. First and foremost, delayed neutron activation analysis is capable of determining multiple fissile nuclide masses within a precision of approximately 5-10% for ^{235}U and ^{239}Pu. This suggests that this method is currently capable of acting as a screening method of evaluating collected materials for concentrations of multiple fissile materials, at concentrations greater than the determination limits given in table 4. This is an important result that will have very meaningful consequences if a large batch of samples ever needs to be processed quickly. Such a scenario is imaginable in the event a large scale nuclear incident, when the quantity of collections would quickly overwhelm the mass spectrometry capabilities of the IAEA Network of Laboratories. This method would allow for samples to be quickly analyzed in order to provide a baseline understanding of the material of analysis. Because DNAA is nondestructive, samples of interest could then be analyzed using more precise techniques, such as mass spectrometry.

The second observation that can be made from this data set is than in instances where m^j is approaching the detection limits of the system, m^i will be overestimated. This seems to be an unavoidable consequence of estimating masses from the linear model and, as seen in sample 1, when a resultant mass of zero is calculated, there is a chance that if there is only an undetectable concentration that other nuclide masses will be overestimated.

Also found in this sample set were the critical, detection, and determination limits for each sample. These results are tabulated below in Table 4.

Table 4. Measured detection limits

	^{235}U			^{239}Pu		
Sample	Critical Limit [ng]	Detection Limit [ng]	Determination Limit [ng]	Critical Limit [ng]	Detection Limit [ng]	Determination Limit [ng]
1	0.0691	0.1722	1.1913	0.1937	0.4828	3.3483
2	0.1122	0.2669	1.475	0.3018	0.7187	3.9847
3	0.0512	0.133	1.0799	0.1465	0.3793	3.0557
4	0.1044	0.25	1.4304	0.2822	0.6766	3.888
5	0.0613	0.1554	1.1588	0.1728	0.4378	3.2494
6	0.0907	0.2199	1.344	0.2466	0.598	3.6486
7	0.0858	0.2093	1.3171	0.233	0.5681	3.5594
8	0.0438	0.1172	1.0524	0.125	0.3331	2.9578
9	0.000587	0.0228	0.7975	0.0016	0.0622	2.1722
10	0.0965	0.2327	1.3822	0.2634	0.6352	3.7728
11	0.000568	0.0228	0.7974	0.0016	0.062	2.1698
12	0.000563	0.0221	0.7734	0.0016	0.0622	2.1752
13	0.1214	0.2869	1.5253	0.3421	0.8083	4.2816
14	0.0811	0.1989	1.2801	0.2319	0.5672	3.6099
15	0.12	0.2841	1.5254	0.3248	0.7696	4.1408
16	0.082	0.201	1.2939	0.2230	0.547	3.527
17	0.0343	0.0959	0.9791	0.0972	0.2716	2.7599

These measured detection capabilities provide insight to the potential applications of this technique. The average determination limit of ^{235}U was found to be 1.20 ng. Similarly, the average determination limit of ^{239}Pu was 3.31 ng. These lower limits of detection were driven by fitting errors to the measured spectrum. For samples that had smaller fitting errors, detection limits improved significantly; ^{235}U had a determination limit of below 1 ng.

Chapter 8

Future Work

The present state of this described delayed neutron activation analysis technique provides a solid foundation for the development of a truly robust nondestructive analytical method for rapidly determining fissile isotopic signatures of special nuclear materials. The refinement of this technique should focus on improving detection capabilities and the expansion of the number of fissile nuclides measurable by this method.

8.1 Secondary Basis Functions

The two primary basis functions are those for ^{235}U and ^{239}Pu, as these two materials are the primary fissile components of any special nuclear material. However, the practical applications of this method rely on the formulation of other, secondary basis functions. Many of the assertions made in developing a mathematical treatment of a delayed neutron emission profile to ascertain individual nuclide masses stipulate that the method is only valid if the model chosen adequately accounts for all possible fissile nuclides in the analyte. The model used in this work has only two basis functions and will only accurately determine ^{235}U and ^{239}Pu in samples that do not contain other fissile constituents. This poses a problem for the analysis of most real-world materials. As such, the next step in the further development of this technique is to account for auxiliary

fissile nuclides that can reasonably be expected to be present in materials that contain ^{235}U or ^{239}Pu, the most imperative of which is ^{241}Pu.

The formulation and incorporation of a ^{241}Pu basis function is a critical next step in the development of this method for two reasons. First, ^{241}Pu is expected to be present at some concentration in all samples that contain measurable quantities of ^{239}Pu. The materials and standards analyzed to date did contain trace amounts of ^{241}Pu, but because of the age of the material and the relatively short half-life of ^{241}Pu of 14.35 years, these concentrations were well below detection capabilities of the method. Not accounting for the presence of all possible fissile plutonium isotopes in an analyzed material, however, will greatly add to the uncertainties of the determined nuclide masses and potentially introduce errors, which may falsify the results. Secondly, plutonium isotopic ratios are an important measurement in many applications of nuclear forensics. This delayed neutron activation analysis technique may very well prove to be the most effective method of determining ^{241}Pu. As a low-energy beta-emitter, ^{241}Pu is inherently difficult to detect and quantify by means other than mass spectrometry. This DNAA method could prove invaluable for the measurement of the $^{241}Pu/^{239}Pu$ ratio. Because of its half-life of only 14.35 years, the $^{241}Pu/^{239}Pu$ ratio provides a potential age-dating mechanism for the assay of unknown nuclear materials. Additionally, the concentration of ^{241}Pu provides insight into not only the burnup of assayed discharged nuclear fuel but also the originally intended use of the plutonium material.

This project has focused on the analysis of material that contains both uranium and plutonium components. Generally speaking, that is to say that these materials

primarily would be derived from one of three sources. Those sources include: discharged light water reactor (LWR) fuels, which produce plutonium as a function of burnup, by the neutron capture reactions of ^{238}U; reprocessed spent nuclear fuel, which can also include fresh mix-oxide fuels; and weapons-grade plutonium, formed by chemically separating plutonium from low-enriched uranium irradiated at low burnups. Like other plutonium isotopes, ^{241}Pu is a common byproduct of the irradiation of ^{238}U. While its production rate in a reactor assembly is significantly lower than that of ^{239}Pu, ^{241}Pu has a thermal fission cross-section of nearly one-and-a-half times that of ^{239}Pu. This is significant in terms of its possible contribution to the delayed neutron emission spectrum of an irradiated sample material. It is also an important stipulation that any material containing ^{239}Pu likely contains ^{241}Pu as well. This is a result of the difficult nature of plutonium isotope separation. Currently, ^{239}Pu enrichment techniques are not capable of complete separation of heavier plutonium nuclides. Consequently, one would expect to find ^{241}Pu in any plutonium sample.

In order to measure ^{241}Pu and to adequately account for its presence in most real-world samples containing ^{239}Pu, a basis function describing the neutron detector response will have to be defined, as was done for ^{235}U and ^{239}Pu. This will require procuring an isotopically certified plutonium reference material containing ^{241}Pu. Of the commercially available plutonium reference materials, even those enriched with respect to ^{241}Pu contain considerable concentrations of ^{239}Pu. However, as long as the ^{239}Pu basis function is defined prior to ^{241}Pu this will not pose any problems. The ^{241}Pu basis function would simply be found as the residual count rate between the expected ^{239}Pu contribution and

the measured delayed neutron emission profile of the irradiated standard. The procedure of determining the ^{241}Pu basis function is similar to the procedure carried out to find the two primary basis functions; however, it remains an important objective in the refinement of this method. Similarly, additional basis functions of other fissile nuclides could be formulated, provided that an appropriate reference material is available.

The utility in developing the capability to quantify other fissile nuclides is particularly apparent in the assay of discharged nuclear fuel, which contains a significant number of anthropogenic fissile nuclides. Contributions to the delayed neutron emission spectrum of an irradiated sample from ^{242m}Am, ^{243}Cm, and other trace fissile constituents of discharged LWR fuel would have to each be accounted for in order for this DNAA technique to be applicable to such complex sample matrices.

There are two practical limitations on adding any secondary basis functions to the model. The first is the availability of an isotopically pure material that can be used to describe the basis function for a given fissile nuclide. Difficulties that have arisen due to the unavailability of an adequate ^{241}Pu material indicate that this is a nontrivial stipulation. The other limitation, as discussed in detail in Chapter 4, is that the delayed neutron intensity regressors for each nuclide must not be collinear, and they must be differentiable within the capabilities of the system. This means that not only must the description functions be independent, but also their differences must be large enough to be resolved by DNAA. The sensitivity of the method to resolve similarly shaped delayed neutron decay curves dictates the eventual limit of this technique. However, this

limitation can be estimated from known delayed neutron emissions data for multiple fissile nuclides.

The limiting sensitivity of DNAA can be expressed as a function of the unaccounted contributors to the delayed neutron emission spectrum. These contributors have been defined previously as the residual errors between the measured spectrum and the fitted basis functions. Generally, these errors are primarily caused by noise in the detector system; other causes are high background radiation incident on the detector array or random processes that cannot be attributed for in the linear model. Consequently, the generalized description of the differences between the neutron emissions profiles must be greater than the detector resolution, defined here as the squared-residual values between the expected and measured neutron emission profiles. This is given as equation 103:

$$\int \hat{P}^i - \int \hat{P}^j > \frac{R^2}{y} \tag{103}$$

where

$\hat{P}^i$ is the normalized basis vector for fissile nuclide *i*

R^2 is the residual errors between the measured and fitted delayed neutron emission spectrum of the mixed nuclide sample

y is the neutron emission factor, as previously defined, to normalize the residuals with respect to total neutrons emitted

The basis vectors must be normalized so that the expected number of neutrons emitted is equivalent for each basis vector, otherwise this expression would not hold true. Because the neutron emissions profiles have yet to have been empirically measured, the

delayed-neutron decay data can be used to approximate the measured delayed neutron spectra for fissile nuclides. Using this data, the normalized emission profile can be expressed as the superposition of the decay of all precursor nuclides, which is often approximated as the sum of six groups

$$\hat{P}^i = \sum_{i=1}^{N} \frac{\beta_i}{\beta} e^{-\lambda_i t} \tag{104}$$

where β_i delayed neutron fraction in the i^{th} delayed neutron group; β is the total delayed neutron fraction, defined as the ratio of the expected number of delayed neutrons to the total neutrons released per fission. This time-depended neutron source expression can be used to determine whether the delayed neutron emission profile of a given irradiated nuclide is sufficiently unique to be resolved by DNAA.

The difference in the expressions is shown in fig 18, below, as the shaded region between the two emissions profiles. Shown here, for illustration purposes is ^{235}U and ^{239}Pu.

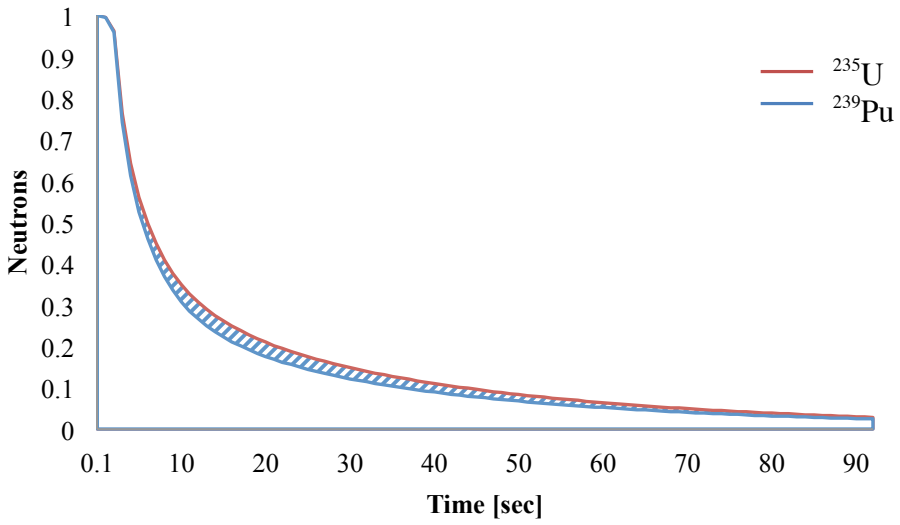

Fig. 18. Difference between ^{235}U and ^{239}Pu delayed neutron emissions profiles

This difference must be greater than the resolution of the detection system; it is not simply enough that the delayed neutron emissions profiles be unique, they must not be so similar that the method cannot distinguish them from one another. Using the linear model to describe the measured neutron response, the error term is the limiting factor in determining the measurement resolution. The relationship between detection error and the difference in the ^{235}U and ^{239}Pu delayed neutron emission profiles are shown in Figure 19.

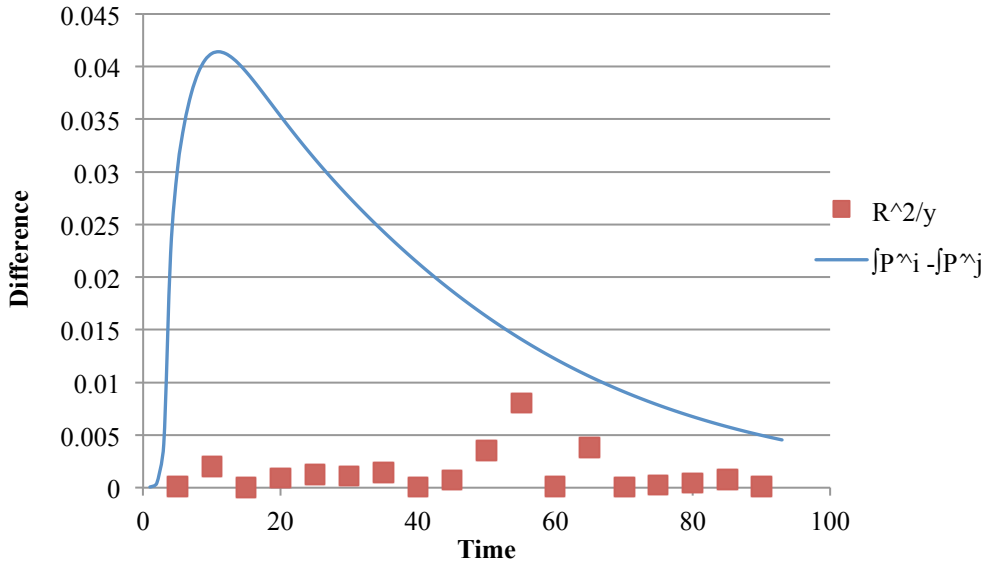

Fig. 19. Detector error and ^{235}U and ^{239}Pu difference

It has been shown that this method is capable of coresolving ^{235}U and ^{239}Pu and the above figure graphically confirms that the curves are sufficiently unique. The satisfaction of this condition will be the primary limiting factor in regards to how many, and which, nuclides will ultimately be analyzed using this DNAA technique.

8.2 Improving Detection Capabilities

Beyond increasing the number of nuclides that can be analyzed using DNAA, the evolution of this project should certainly explore methods of improving lower limits of detection. Fundamentally, in order to improve detection capabilities, methods must be explored that ultimately improve the neutron-counting statistics. Because irradiations were performed using one of the highest steady-state neutron fluxes in the world and the

samples were irradiated to greater than 95% saturation, there are a limited number of approaches available to generate an increased delayed neutron signal to improve the counting statistics. However, advanced irradiation techniques, such as employing cyclic irradiations and summing multiple delayed neutron spectra, should in the future be explored. Cyclic delayed neutron activation analysis (CDNAA) has been explored as a method of increasing the measured signal-to-noise ratio for the analysis of single fissile nuclides (83).

Noise reduction methods have been employed in this work, and have been previously discussed. The thorough optimization of detector components completed to date indicate that they are no obvious solutions to reducing the spectrum noise and reducing errors; however, further error reduction should be explored. A conscious effort was made to develop this technique avoiding signal manipulation, such as signal averaging or advanced signal smoothing algorithms. The motivation for avoiding such methods was to develop a DNAA technique that does not reply on curve fitting or other data manipulation, in order to demonstrate the validity of the regression model. Having shown that formulated method is valid, future efforts may choose to implement some other signal smoothing techniques.

Finally, the decay time uncertainty must be addressed. Having to iteratively solve the model from a range of possible basis functions because of sample decay time variability led to increased uncertainties in the measurements. The simplest solution would be to couple monitors to the pneumatic transfer system tubes so that it can be observed when the sample leaves the reactor core (the end of irradiation) and when it

arrives to the detector array. This would provide the capacity to correct for variances in sample decay time.

8.4 Signature Development

Finally, there needs to be work that will ultimately create utility of the method. Once detection limits are improved, and other nuclides are capable of being measured, the specific isotopic ratios of greatest interest that can be measured by this method need to be defined. If the greatest utility of this DNAA method is to attribute derivatives of discharged nuclear fuel, then expected isotopic signatures that can be used to identify initial fuel composition or reactor type must be found in order to fully appreciate the utility in this method.

Chapter 9

Conclusions

The DNAA technique described here represents a new and powerful nondestructive analytical method for evaluating the fissile isotopic composition of special nuclear materials. A method of analyzing a single delayed neutron emission profile following irradiation at ORNL's High Flux Isotope Reactor has been developed for the quantification of each of the contributory fissile components in a sample.

The goal of this work was to address the imminent need for a fast and reliable analytical method for the assay of nuclear material; current analytical techniques rely too heavily on destructive methods, which are laborious and time intensive. To develop such a technique, this work sought to revisit the notion that delayed neutron activation analysis is capable only of quantifying fissile nuclides in samples containing only one fissile component. The existing delayed neutron counting facility at HFIR was modified so that a time resolved delayed neutron emission profile of irradiated samples could be recorded. The acquired delayed neutron spectrum was then mathematically described as a linear combination of βn-decay of each contributing fissile component. As such, ordinary least squares regression was then employed to estimate the masses of each fissile component present in the sample.

In order to validate and substantiate the described method, DNAA and the postulated spectral analysis was performed to quantify trace concentrations of ^{235}U and

^{239}Pu in a series of samples prepared using isotopically certified standard reference materials. Appropriate basis functions were formulated for ^{235}U and ^{239}Pu and incorporated into a multielement regression model. Samples containing various concentrations of ^{235}U and ^{239}Pu were irradiated and analyzed. This experiment set confirmed the validity of the described method. The measured nuclide masses agreed with the known nuclide masses, generally with a precision of within 5%. Further, expressions for the detection, critical, and determination limits were derived from Curie detection limits. As evident by the lowest concentration samples, the calculated determination adequately described the limiting concentrations of fissile material.

The validation experiment demonstrated conclusively that the delayed neutron emission spectrum can be defined as a linear combination of the neutrons emitted from each fissile component. As long as the delayed neutron emission profiles are sufficiently unique, additional fissile nuclides can be integrated into the linear model. However, in its present state, the DNAA method has been able to resolve ^{235}U and ^{239}Pu in binary mixtures of uranium and plutonium without the arduous sample preparation required by commonly employed destructive methods.

New, rapid analytical techniques must continually be developed to augment the destructive analytical methods relied on in many facets of nuclear forensics. The need for quicker and simpler analytical techniques is currently apparent in the routine analysis of environmental swipe samples, but will be exacerbated in the event of a large-scale nuclear event, when the quantity of samples would quickly overwhelm the mass spectrometry capabilities of the IAEA Network of Laboratories.

As such, the immediate applications of this method should begin with the IAEA swipe samples currently being analyzed using a classic application of DNAA, and was incapable of analyzing samples containing multiple fissile components. The protocol for analyzing environmental swipe samples will be greatly improved with the integration of this new technique. By not limiting the samples to those that contain only a single fissile nuclide, not only will this allow for a broader scope of materials and samples to be analyzed, but it would provide greater confidence the results of the samples that contain only a single fissile component. This confidence comes from knowing that a second unknown fissile component is not present to obscure the measurements. While the implementation of this technique will be greatly beneficial to the efforts at HFIR, the utility of this method is not limited to the NAA lab at ORNL.

This DNAA technique can easily be incorporated at other reactor facilities. The procedure to retrofit and adapt the previous delayed neutron counting facility was straightforward and required only a few modifications to the existing hardware. The installation of the ORTEC multichannel scaler was a cost effective and simple addition, which allowed for the time resolved delayed neutron profile to be digitalized so that it could seamlessly be imported into MATLAB for analysis.

As this technique is implemented at ORNL and elsewhere, further application, capabilities, and limitations will be realized. What is for certain at this point is that it is incumbent upon the scientific community to provide analytical measurements with a level of certainty at a timeliness that is not currently attainable with destructive methods.

The need for more advanced analytical methods is accentuated by the expansion of nuclear technology all over the world. The analysis of both interdicted nuclear materials and effluents collected at nuclear materials processing facilities provides the basis for nuclear security and nonproliferation policy. The inherently difficult nature of the currently employed destructive analytical methods limits the timescales that that information is ascertained, and consequently, how quickly important decisions can be made. This novel application of DNAA has the potential to greatly advance the analytical capabilities of the nuclear forensics community.

REFERENCES

1. *Can the NPT Survive? The Theory and Practice of US Nuclear Non-proliferation Policy after September 11*. **Carranza, M. E.** 2006, Contemporary Security Policy, Vol. 27, pp. 489-525.

2. *Contextualizing Past, Present and Future Challenges to the NPT Regime*. **Tyson, R.** 2004. Disarmament Forum. Vol. 4, pp. 57-67.

3. *Analytical Atomic Spectrometry for Nuclear Forensics*. **Hou, X. Chen, W., He, Y., Jones, B. T.** 2005, Appl. Spectro. Rev., Vol. 40, pp. 245-247.

4. **Dunlop, W.H., Smith, H. P.** *Who Did It? Using International Forensics to Detect and Deter Nuclear Terrorism*. Lawrence Livermore National Laboratory. 2006.

5. *Before the Day After: Using Pre-Detonation Nuclear Forensics to Improve Fissile Material Secuity*. **Chivers, D. H., Lyles Goldblum, B.F., Isselhardt, B. H., Snider, J. S.** 2008, Arms Control Today, pp. 22-28.

6. *Origin determination of plutonium material in nuclear forensics*. **Wallenius, M., Peerani, P., Koch, L.** 2000, J. Radioanal. Nucl. Chem, Vol. 246, pp. 317-321.

7. *Nuclear forensic science-From cradle to maturity*. **Mayer, K., Wallenius, M., Fanghaenel, T.** 2007, J. Alloys and Comp., Vol. 444, pp. 50-56.

8. *Illicit nuclear trafficking in the NIS: What's new? What's true?* **Potter, W.C., Sokova, E.** 2002, Nonprolif. Review, pp. 112-120.

9. *Environmental and Source Monitoring for Purposes of Radiation Protection*. International Atomic Energy Agency. Vienna : s.n., 2005.

10. **Kuhn, E., D. Fischer, M. Ryjinski.** *Environmental Sampling for IAEA Safeguards: A Five Year Review*. Vienna : s.n., 2001.

11. **Vogt, S., P. Zahradnik, D. Klose, H. Swietly.** *Bulk Analysis of Environmental Swipe Samples*. IAEA. Seibersodorf, Austria : s.n., 2001.

12. *The use of SIMS and SEM for the characterization of individual particles with a matrix originating from a nuclear weapon*. **Ranebo, Y., Eriksson, M., Tamborini, G., Niagolova, N., Bildstein, Ol., Betti, M.** 2007, Microscopy and Microanal., Vol. 13, pp. 179-190.

13. *Use of secondary ion mass spectrometry in nuclear forensic analysis for the characterization of plutonium and highly enriched uranium particles*. **Betti, M., Tamborini, G., Koch, L.** 1999, Anal. Chem., Vol. 71, pp. 2616-2622.

14. *Investigation of the isotopic composition of lead and trace elements concentrations in natural uranium materials as a signature in nuclear forensics*. **Svedkrauskaite-LeGore, J., Mayer, K., Millet, S., Nicholl, A., Rasmussen, G., Baltrunas, D.** 2007, Radiochim. Acta., Vol. 95, pp. 601-605.

15. *Applications, Development of a SIMS method for isotopic measurements in nuclear forensics*. **Tamborini, G., Wallenius, M., Bildstein, Ol., Pajo, L., Betti, M.** 2002, Microchimica Acta., Vol. 139, pp. 185-188.

16. *Application of secondary ion mass spectrometry to the identification of single particles of uranium and their isotopic measurement*. **Tamborini, G., Betti, M., Forcina, V., Hiernaut, T., Giovannone, B., Koch., L.** 1998, Spectrochimica Acta B, Vol. 53, pp. 1289-1302.

17. *Isotope ratio analysis of actinides, fission products, and geolocators by high-efficiency multi-collector thermal ionization mass spectrometry*. **Buerger, S., Riciput, L. R., Bostick, D. A., Turgeon, S., McBay, E.H., Lavelle, M.** 2009, Internat. J. Mass. Spectrom., Vol. 286, pp. 70-82.

18. *Development of activation techniques for extensive requirement in uranium and multielement analysis*. **Papadopoulos, N. N.** 1987, J. Radioanal. Nucl. Chem, Vol. 113, pp. 351-356.

19. *Delayed neutrons from U-235 after short irradiation*. **DeHoffman, F., Feld, B. T., Stein, P. R.** Phys. Rev.1948, Vol. 74, pp. 1330-1337.

20. *Uranium concentrations in marine sediments*. **Mo, T., Suttle, A. D., Sackett, W. M.** 1973, Geochim. Cosmochim. Acta, Vol. 37, pp. 35-51.

21. *An automated delayed neutron counting system for mass determinations of special nuclear materials*. **Sellers, M. T., Kelly, D. G., Corcoran, E. C.** 2012, J. Radioanal. Nucl. Chem, Vol. 291, pp. 281-285.

22. *Isotope ratio analysis of actinides, fission products, and geolocators by high-efficiency multi-collector thermal ionization mass spectrometry*. **Buerger, S., et al.** 2009, Int. J. Mass Spectrom., Vol. 286, pp. 72-80.

23. *Nuclear forensics in law enforcement applications*. **Grant, P.M., et al.** 1998, J. Radioanal. Nucl. Chem, Vol. 235, pp. 129-132.

24. *Detection of previous neutron irradiation and reprocessing of uranium materials for nuclear forensics purposes*. **Vargha, Z., Suranyi, G.** 2009, Appl. Rad. Iso., Vol. 67, pp. 516-522.

25. *Application of isotopic fingerprinting in nuclear forensic investigations: a case study*. **Mayer, K., et al.** Karlsruhe : IAEA, 2002. Advances in Destructive and Non-destructive Analysis for Environmental Monitoring and Nuclear Forensics. IAEA-CN-98/11.

26. *Experience with Environmental Swipe Sampling in a Newly Build Gas Centrifuge Plant*. **Cooley, J., et al.** Phoenix : s.n., 1999. Proc of the 4th Annual Meetin gof the Institute of Nuclear Materials Management.

27. *IAEA Experience with Environmental Sampling at Gas Centrifuge Enrichment Plants in the European Union*. **Bush, W., et al.** Vienna : s.n., 2001. Proc. Symp. on International Safeguards, Verification and Nuclear Material Security.

28. *Secondary ionization mass spectrometric analysis of impurity element isotope ratios in nuclear reactor materials*. **Gerlach, D.C., et al.** 2006, Appl. Surf. Sci., Vol. 252, pp. 7041-7044.

29. *Analysis of high burnup spent nuclear fuel by ICP-MS*. **Wolf, S. F., Bowers, D. L., Cunnane, J.C.** 2005, J. Radioanal. Nucl. Chem., Vol. 263, pp. 581-586.

30. **Guenther, R. J., et al.** *Characterization of Spent Fuel Approved Testing Material*. s.l. : Pacific Northwest Laboratory Report, 1988.

31. *U, Pu, and Am Nuclear Signatures of the Thule Hydrogen Bomb Debris*. **Eriksson, M., Lindahl, P., Roos, P., Dahlgaard, H., Holm, E.** 2008, Environ. Sci. Technol., Vol. 42, pp. 4717-4722.

32. *Iran at the Nuclear Threshold*. **Shaffer, B.** 2003, Arms Control Today

33. *Theoretical Mechanism Study of UF6 Hydrolysis in the Gas Phase*. **Hu, S., Wang, X., Chu, T., Liu, X.** 2008, J. Phys. Chem. A, Vol. 112, pp. 8877-8883.

34. *Conclusions on plutonium separation from atmospheric krypton-85 measured at various distances from Karlsruhe reprocessing plant*. **Kalinowski, M., Sartorius, H., Uhl, S., Weiss, W.** 2004, J. Env. Radioact., Vol. 73, pp. 203-222.

35. *The basics of mass spectrometry in the twenty-first century*. **Glish, G. L., Vachet, R. W.** 2003, Nat. Rev. Drug Disc., Vol. 2, pp. 140-150.

36. *Feasibility study of isotope ratio analysis of individual uranium-plutonium mixed oxide particle with SIMS and ICP-MS*. **Esaka, F., et al.** 2011, Mass Spectrom. Lett., Vol. 4, pp. 80-83.

37. *Analysis of IAEA environmental samples for plutonium and uranium by MCP/MS in support of international safeguards*. **Farmer III, O. T., Olsen, K. B., Thomas, M. L., Garofoli, S. J.** 2008, J. Radioanal. Nucl. Chem, Vol. 276, pp. 489-492.

38. *Production and characterization of monodisperse plutonium, uranium, and mixed uranium-plutonium particles for nuclear safeguards application*. **Ranebo, Y., et al.** 2010, Anal. Chem., Vol. 82, pp. 4055-4062.

39. *Isotopic analysis of single uranium and plutonium particles by chemical treatment and mass spectrometry*. **Shinonaga, T., Esaka, F., Magara, M., Klose, D., Donohue, D.** 2008, Spectrochim. Acta, Part B, Vol. 63, pp. 1324-1328.

40. *Characterization of uranium and plutonium in surface-waters and sediments collected at the Rocky Flats Facility*. **Efurd, D.W., et al.** San Diego : s.n., 1994. Sym. on Applications of Nuclear Chemistry, ACS.

41. *Accelerator mass spectrometry of plutonium isotopes*. **Fifield, L. K., et al.** 1996, Nucl. Instr. and Meth. B, Vol. 117, pp. 295-303.

42. *Determination of plutonium from different sources in environmental samples using alpha-spectrometry and AMS*. **Bisinger, T., Hippler, S., Michel, R., Wacker, L., Synal, H.-A.** 2010, Nucl. Inst. Meth. B, Vol. 268, pp. 1269-1272.

43. *Isotopic analysis of uranium and plutonium mixtures by resonance ionization mass spectrometry*. **Donohue, D. L., Smith, D. H., Young, J. P., McKown, H. S., Pritchard, C. A.** 1984, Anal. Chem., Vol. 56, pp. 379-381.

44. *Verification of a Fissile Material Cutoff Treaty: The case of enrichment facilities and the role of ultra-trace level isotope ratio analysis*. **Glaser, A., Buerger, S.** 2009, J. Radioanal. Nucl. Chem, Vol. 280, pp. 85-90.

45. *Measurement of trace uranium isotopes using a porous ion emitter*. **Watrous, M. G., Delmore, J.E.** 2011, Int. J. Mass Spectrom., Vol. 303, pp. 1-5.

46. *Thermal ionization mass spectrometry of uranium with electrodepostion as a loading technique*. **Rokop, D. J., et al.** 1982, Anal. Chem., Vol. 54, pp. 957-960.

47. *Resonance Ionization Mass Spectrometry*. **Young, J. P., Shaw, R. W., Smith, D. H.** 1989, Anal. Chem, Vol. 61, pp. 1271-1276.

48. *Isotopic Analysis of Uranium and Plutonium Mixtures by Resonance Ionization Mass Spectrometry*. **Donohue, D. L., et al.** 1984, Anal. Chem., Vol. 56, pp. 379-381.

49. *Accelerator mass spectrometry of actinides*. **Marchetti, A. A., Brown, T. A., Cox, C. C., Hamilton, T. F., Martinelli, R. E.** 2005, J. Radioanal. Nucl. Chem, Vol. 263, pp. 483-487.

50. **McWade, Laura.** Accelerator Mass Spectrometry. [Online] UC Davis, 2010. http://chemwiki.ucdavis.edu/Wikitexts/UCD_Chem_205%3A_Larsen/ChemWiki_Module_Topics/Accelerator_Mass_Spectroscopy.

51. *Accelerator mass spectrometry of plutonium isotopes*. **Fifield, L. K., et al.** 1996, Nucl. Instr. Meth. B, Vol. 117, pp. 295-303.

52. *Nuclear forensic investigations: Two case studies*. **Wallenius, M., Mayer, K., Ray, I.** 2006, Forensic Sci. Internat., Vol. 156, pp. 55-62.

53. *Production of monodisperse uranium oxide particles and their characterization by scanning electron microscopy and secondary ion mass spectrometry*. **Erdmann, N., Betti, M., Stetzer, O., Tamborini, G., Kratz, J.V., Trautmann, N., van Geel, J.** 2000, Spectrochim. Acta B, Vol. 55, pp. 1565-1575.

54. *Basic characterization of highly enriched uranium by gamma spectrometry*. **Nguyen, C. T., Zsigrai.** 2006, Nucl. Instr. Meth. Phys. Res., Vol. 246, pp. 417-424.

55. *Analysis of nuclear material by alpha spectroscopy with a transition-edge microcalorimeter*. **Horansky, R. D., et al.** 2008, J. Low Temp. Phys., Vol. 151, pp. 1067-1073.

56. *State-of-the-art and progress in precise and accurate isotope ratio measurements by ICP-MS and LA-ICP-MS*. **Becker, J.S.** 2002, J. Anal. Atom Spectrom., Vol. 17, pp. 1172-1185.

57. *Strengthening IAEA safeguards through environmental sampling and analysis*. **Donohue, D.L.** 1998, J. Alloys. Comp., Vol. 271, pp. 11-18.

58. *Production date determination of uranium-oxide materials by inductively coupled plasma mass spectrometry*. **Varga, Z., Suranyi, G.** 2007, Anal. chim. Acta., Vol. 599, pp. 16-23.

59. *Comparison of active and passive environmental sampling for safeguards applications*. **Cable-Dunlap, P., et al.** 2012, J. Radioanal. Nucl. Chem, p. In Press.

60. **Donohue, D.** *Environmental sample analysis-Advances and future trends*. IAEA. Vienna, Austria : s.n., 2010.

61. **Faure, G., T. M. Mensing.** *Isotopes: Principles and Applications*. [ed.] Third. Hoboken : John Wiley & Sons, 2005. pp. 48-49.

62. **Egnatuk, C.** *Identifying short-lived fission products by delayed gamma-ray emission*. The University of Texas at Austin. 2009. Master's thesis.

63. **Kunzendorf, H., L. Lovborg, E. M. Christiansen.** *Automated Uranium Analysis by Delayed-Neutron Counting*. Riso National Laboratory. Roskilde, Denmark : s.n., 1980.

64. *Systematics of neutron emission probabilities from delayed neutron precursors*. **Kratz, K.L., G. Herrmann.** 1973, Z. Physik, Vol. 263, pp. 435-442.

65. **Nichols, A. L., D. L. Aldama, M. Verpelli.** *Handbook of Nuclear Data for Safeguards: Database Extensions, August 2008*. International Atomic Energy Agency. Vienna : s.n., 2008.

66. *Rapid determination of uranium and plutonium content in mixtures through measurement of the intensity-time curve of delayed neutrons*. **Li, X., R. Henkelmann, F. Baumgartner.** 2004, Nucl. Inst. and Meth. in Phys Res. B, Vol. 215, pp. 246-251.

67. *The Gauss-Markov Theorem for regression models with possibly singular covariances*. **Albert, A.** 1973, J. Appl. Math., Vol. 24, pp. 182-187.

68. *A generalization of the Gauss-Markov Theorem*. **Lewis, T. O., Odell, P. L.** 1966, J. Am. Stat. Assoc., Vol. 61, pp. 1063-1066.

69. **Wooldridge, Jeffery M.** *Introductory Econometrics: A Modern Approach*. s.l. : South-Western College Publishing, 2000.

70. *The Lagrange Multiplier Test and its applications to model specification in econometrics*. **Breusch, T.S., Pagan, A. R.** 1980, Rev. Econ. Stud., Vol. 47, pp. 239-253.

71. *A note on algebraic equivalence of White's test and a variation of the Godfrey/Breusch-Pagan test for heteroscedasticity*. **Waldman, D. M.** 1983, Econ. Lett., Vol. 13, pp. 197-200.

72. *Characterization of a BNCT beam using neutron activation and indirect neutron radiography*. **Tsai, P., et al.** 2010, Rad. Meas., Vol. 45, pp. 1167-1170.

73. *Limits for Qualitative Detection and Quantitative Determination*. **Currie, L. A.** 1968, Anal. Chem., Vol. 40, pp. 586-593.

74. **Lindstrom, R. M.** *Limits for Qualitative Detection and Quantitative Determination*. s.l. : NIST Special Publications, 2001. pp. 164-166.

75. *Terrestrial Thermal Neutrons*. **Dirk, J. D., et al.** 2003, IEEE Trans. Nucl. Sci, Vol. 50, pp. 2060-2064.

76. *Improved performance of BF3 neutron counters in high gamma fluxes*. **Stokes, A. J.** 1966, IEEE Trans. Nucl. Sci, Vol. 13, pp. 630-635.

77. *Neutron detection alternatives to 3He for national security applications*. **Kouzes, R. T., et al.** 2010, Nucl. Instr. Meth. Phys. Res., Vol. 623, pp. 1035-1045.

78. **Ellison, S.L.R, Rosslein, M., Williams, A. (eds).** *Quantifying Uncertainty in Analytical Measurement*. s.l. : Eurachem, 2000.

79. *Pushing the limits of NAA: Accuracy, uncertainty and detection limits*. **Greenberg, R.R.** 2008, J. Radioanal. Nucl. Chem, Vol. 278, pp. 231-240.

80. *Determination of Hg and other trace elements in soil using neutron activation analysis*. **Robinson, L., et al.** 1994, J. Radioanal. Nucl. Chem., Vol. 179, pp. 305-313.

81. *Determination of uranium and thorium in semiconductor memory materials by high fluence neutron activation analysis*. **Dyer, FF, JF Emery, KJ Northcutt, RM Scott.** J. Radioanal. Nucl. Chem, Vol. 72, pp. 53-67.

82. **Dyer, FF, et al.** *A comprehensive study of the neutron activation analysis of uranium by delayed neutron counting*. 1962.

83. *Assay of fissile materials by a cyclic method of neutron activation analysis*. **MacMurdo, K. W., Bowman, W. W.** 1977, Nucl. Instr. Meth., Vol. 141, pp. 299-306.

84. *Robust tests for heteroscedasticity based on regression quantiles*. **Koenker, R., Bassett, G.** 1982, Economet., Vol. 50, pp. 43-61.

85. *Assay of fissile materials by a cyclic method of neutron activation and delayed neutron counting*. **MacMurdo, K. W., Bowman, W. W.** 1977, Nucl. Instr. Meth, Vol. 141, pp. 299-306.

Vita

Roger Kapsimalis grew up in Columbus, NJ where he attended Springfield Township schools and graduated from Northern Burlington County Regional High School. He then enrolled at The University of Texas in Austin in the fall of 2004. After receiving a BS in Physics, Roger remained at UT where he joined the Nuclear and Radiation Engineering Program. He earned his MSE in 2010 for his work with the Neutron Radiography Facility at Sandia National Laboratories. While continuing his doctoral research, Roger took a postmaster's appointment at Oak Ridge National Laboratory in 2011, working in the Nuclear Forensics Thrust Area under Dr. Brian Anderson.

While Texas is still the place he'd dearly love to be, following the advice of George Strait, Roger now resides in Tennessee.

Permanent Address

9501 Thronhill Way #317
Knoxville, TN 37931

This dissertation was typed by the author